Oil-palm management alters the spatial distribution of amorphous silica and mobile silicon in topsoils

Britta Greenshields[1], Barbara von der Lühe[1*], Harold J. Hughes[1], Christian Stiegler[2], Suria Tarigan[3], Aiyen Tjoa[4], Daniela Sauer[1]

[1]Department of Physical Geography, University of Göttingen, Göttingen, 37077, Germany
*Now at the Faculty of Geoscience, University of Münster, Münster, 48149, Germany
[2]Bioclimatology, Büsgen Institute, University of Göttingen, Göttingen, 37077, Germany
[3]Department of Soil and Natural Resources Management, IPB University, Dramaga Bogor, 16680, Indonesia
10 [4]Department of Agrotechnology, Tadulako University, Palu, 94118, Indonesia

Correspondence to: Britta Greenshields (britta.greenshields@uni-goettingen.de)

Abstract. Effects of oil-palm (*Elaeis guineensis* Jacq.) management on silicon (Si) cycling under smallholder oil-palm plantations have hardly been investigated. As oil palms are Si accumulators, we hypothesized that
15 management practices and topsoil erosion may cause Si losses and changes in spatial Si concentration patterns in topsoils under oil-palm cultivation. To test this hypothesis, we took topsoil samples under mature oil-palm plantations in well-drained and riparian areas of Jambi Province, Indonesia. The samples were taken from four different management zones within each oil-palm plot: palm circles, oil-palm rows, interrows and below frond piles. We quantified mobile Si (Si_M) and Si in amorphous silica (Si_{Am}) by $CaCl_2$ and $NaCO_3$ extraction,
20 respectively. Both fractions are important Si pools in soils and are essential for plant-soil Si cycling. We further installed sediment traps on sloping, well-drained oil-palm plantations to estimate the annual loss of soil and Si_{Am} caused by erosion. In well-drained areas, mean topsoil Si_{Am} concentrations were significantly higher below frond piles (3.97 ±1.54 mg g^{-1}) compared to palm circles (1.71± 0.35 mg g^{-1}), oil-palm rows (1.87 ± 0.51 mg g^{-1}) and interrows (1.88 ± 0.39 mg g^{-1}). In riparian areas, highest mean topsoil Si_{Am} concentrations were also found below
25 frond piles (2.96 ± 0.36 mg g^{-1}) and in grass-covered interrows (2.71 ± 0.13 mg g^{-1}), whereas topsoil Si_{Am} concentrations of palm circles were much lower (1.44 ± 0.55 mg g^{-1}). We attributed the high Si_{Am} concentrations in topsoils under frond piles and in grass-covered interrows to phytolith release from decaying oil-palm fronds, grasses, and sedges. The significantly lower Si_{Am} concentrations in palm circles (in both well-drained and riparian areas), oil-palm rows and unvegetated interrows (only in well-drained areas) were explained by a lack of litter
30 return to these management zones. Mean topsoil Si_M concentrations were in a range of ~10 – 20 µg g^{-1}. They tended to be higher in riparian areas, but the differences between well-drained and riparian sites were not statistically significant. Soil-loss calculations based on erosion traps confirmed that topsoil erosion was considerable in oil-palm interrows on slopes. Erosion estimates were in a range of 4 – 6 Mg ha^{-1} yr^{-1}, involving Si_{Am} losses in a range of 5 – 9 kg^{-1} ha^{-1} yr^{-1}. Based on the observed spatial Si patterns, we concluded that
35 smallholders could efficiently reduce erosion and support Si cycling within the system by (1) maintaining a grass cover in oil-palm rows and interrows, (2) incorporating oil-palm litter into plantation management and (3) preventing soil compaction and surface-crust formation.

Keywords: oil-palm plantations, oil-palm management, silicon pools, phytoliths, topsoil erosion, silicon extraction

1 Introduction

Lowland-rainforest transformation to cash-crop plantation systems (e.g., timber, rubber, and oil palm) involves vast expansion of oil-palm monocultures in Jambi Province, Indonesia (Drescher et al., 2016; Tsujino et al., 2016). By now, smallholder farmers manage 40 % of oil-palm plantations in Jambi Province (Euler et al., 2016), whereby palm oil remains a tropical cash crop with high demand on the global market (FAO 2020). Oil-palm cultivation has improved the livelihoods of many smallholder farmers, yet at the expense of the natural environment (Clough et al., 2016; Grass et al., 2020; Qaim et al., 2020), leading to a decrease in biodiversity (Drescher et al., 2016; Meijaard et al., 2020) and ecosystem services (Dislich et al., 2017). Due to these "trade-offs" (Grass et al., 2020) and a global interest to reduce deforestation (Tsujino et al., 2016), much research focuses on identifying ways to increase land-use sustainability while keeping current oil-palm plantations profitable (Darras et al., 2019; Luke et al., 2019).

Under humid-tropical climate conditions, intense silicate weathering and element leaching from soils takes place, including leaching of silicon (Si), *i.e.*, desilication (Haynes, 2014). Farmers commonly apply nitrogen-phosphorous-potassium (NPK) fertilizers and lime to maintain an adequate plant nutrition and soil pH (Darras et al., 2019). However, Si also plays an important role in terrestrial biogeochemical cycling (Struyf and Conley, 2012) and enhances crop production in several ways (Epstein, 2009; Guntzer et al., 2012). In soils, silicic acid can mobilize phosphate by occupying anion adsorption sites. Si also mitigates plant toxicity by binding toxic cations such as aluminium (Al), cadmium (Cd), and arsenic (As) that become mobile at low soil pH (Street-Perrott and Barker, 2008; Schaller et al., 2020). Furthermore, Si can increase drought resistance of plants (Schaller et al., 2020). Silica precipitates in cell walls, cell lumen and intercellular spaces of leaves and can reduce transpiration (Epstein, 2009). In Si-depleted soils, some crops, including oil palms, can thus benefit from Si fertilization (Klotzbücher et al., 2018).

In terrestrial ecosystems, Si cycling is mostly driven by two Si pools: mobile Si in soil solution (Si_M) and Si present in amorphous silica (Si_{Am}) (Struyf et al., 2010; de Tombeur et al., 2020). Si_M is the Si fraction that is readily available to plants and usually present as monomeric silicic acid (H_4SiO_4) in terrestrial environments (Georgiadis et al., 2013). Si_{Am} is the largest non-mineral Si pool in soils (Barão et al., 2014; Unzué-Belmonte et al., 2017). Its solubility exceeds that of silicate minerals by several orders of magnitude (Iler, 1979; Fraysse et al., 2009). Si_{Am} in soils can be subdivided into Si_{Am} of biogenic origin and of pedogenic origin. The first mainly includes Si in phytoliths, *i.e.*, small bio-opal bodies precipitated in plant tissues that are released during plant-litter decomposition (Barão et al., 2014; Clymans et al., 2015; Schaller et al., 2021). Soil microorganisms (testate amoebae, sponges, diatoms) contribute to a lesser extent (Schaller et al., 2021). Si_{Am} of pedogenic origin, *i.e.*, silica precipitated from soil solution, mainly occurs as soil-particle coatings and void infillings (Schaller et al., 2021). Si_{Am} in topsoils is predominantly of biogenic origin (Clymans et al., 2015; Schaller et al., 2021), whereas Si_{Am} in subsoils is mostly of pedogenic origin (Schaller et al., 2021).

Ecosystem Si cycling can be altered by human impact such as deforestation (Conley et al., 2008), land-use/land-cover (LULC) change (Struyf et al., 2010; Barão et al., 2020), and fire (von der Lühe et al., 2020; Schaller and Puppe, 2021). After LULC transformation from forest to arable land, Si can be lost from the system through harvest, topsoil erosion, and increased soil Si leaching. Soil Si leaching is triggered by reduced interception, which results in increased percolation (Keller et al., 2012; Vandevenne et al., 2012; Kraushaar et al., 2021). Si-

accumulating plants such as rice, wheat, barley, maize, and oil palm (Ma and Takahashi, 2002; Munevar and Romero, 2015), are characterized by Si accumulation of > 1 wt. % in dry leaf tissue and a Si/Ca ratio > 1 (Ma and Takahashi, 2002). Such Si accumulators may accelerate Si turnover at the soil-plant interface by taking up high amounts of Si from soil solution and returning Si-rich litter to soils (Struyf and Conley, 2009, 2012). In oil-palm plantations, we therefore expected Si losses by harvest and topsoil erosion (Vandevenne et al., 2012; Munevar and Romero, 2015). In addition, we expected that the spatial arrangement of oil-palms rows and interrows – with frond piles (frond pile) or without ("empty" interrow) – results in a corresponding spatial Si concentration pattern in topsoils.

Oil palms are planted in rows (Kotowska et al., 2015) (Fig. 1a). A distance is kept between the rows to ensure sufficient light exposure (Corley and Tinker, 2016). The space between two oil-palm rows is referred to as an interrow. They either serve as harvesting paths or as deposition sites for cut-off palm fronds that are stacked up in long, flat piles (Corley and Tinker, 2016). Fertilizers are only applied within a circle of ~1.5 – 2 m around the palm stem (palm circle) (Munevar and Romero, 2015; Formaglio et al., 2020). In addition, nutrients are released from decaying plant litter. Thus, we hypothesized that Si is mainly released and returned to soils in the form of biogenic Si_{Am} under frond piles, leading to higher topsoil Si_{Am} concentrations, while other management zones (including palm circles, oil-palm rows and "empty" interrows) might be at risk of Si depletion.

Furthermore, we hypothesized that in oil-palm plantations established on sloping terrain, Si is removed by topsoil erosion in scarcely vegetated interrows. We assumed that phytoliths might be even more prone to erosion than mineral soil particles because of their lower density, leading to a disproportionately high Si_{Am} loss through topsoil erosion. Such additional Si_{Am} loss from interrows would be unfavourable, as interrows may serve as new planting sites in a subsequent plantation cycle after ~25 years (Corley and Tinker, 2016). Thus, our study aimed at assessing the impact of management practices in smallholder oil-palm plantations on Si cycling. In addition, we considered it important to account for potential differences in the intensity of natural desilication in different landscape positions. Therefore, we carried out the same study in two different landscape positions, associated with differing water regimes: in well-drained areas with presumably high desilication rates, and riparian areas, where we assumed that regular flooding might involve an input of Si dissolved in stream water into the system, partially compensating for desilication.

2 Material and Methods

2.1 Study area and sites

The study was associated to the DFG-funded interdisciplinary Collaborative Research Centre CRC 990, addressing environmental and socioeconomic impacts of rainforest conversion into plantation systems in Sumatra, Indonesia (Drescher et al., 2016; Dislich et al., 2017). Thus, it was conducted on CRC 990 plots in smallholder oil-palm plantations in the Harapan landscape of Jambi Province, Sumatra, Indonesia (1° 55' 0'' S, 103° 15' 0'' E; 50 m ± 5 m NN). Geologically, this lowland landscape is characterised by pre-Paleogene metamorphic and igneous bedrock that is overlain by lacustrine and fluvial sediments (de Coster, 2006), in which predominantly loamy mineral soils have formed (Allen et al., 2016). Preliminary results showed that quartz, kaolinite, and Fe-Al-oxides are the most abundant minerals in these highly weathered soils. In our study area, Acrisols are present in well-drained areas, found at higher elevation and on sloping terrain. Stagnosols and Stagnic Acrisols dominated in seasonally flooded riparian plots, *i.e.*, in floodplains (Hennings et al., 2021). The Harapan region is characterised

by a humid-tropical climate (Af in the Köppen-Geiger classification) with a mean annual temperature of 26.7 °C and a mean annual precipitation of 2230 mm (Drescher et al., 2016). The rainy season has two precipitation maxima: one in December and another one in March. A dry period lasts from July to August (Drescher et al., 2016). The natural vegetation is mixed dipterocarp lowland rainforest (Laumonier, 1997), which is nearly only preserved in the Harapan rainforest, an ecosystem restoration area in the South of Jambi Province (Harrison and Swinfield, 2015), and in the Barisan mountains in the West of Jambi Province (Drescher et al., 2016). In addition to oil-palm plantations, other important land-use systems in Jambi Province include rubber plantations and agroforestry systems (Dislich et al., 2017).

2.2 Study design and sampling

2.2.1 Topsoil samples

From April to August 2018, topsoil sampling was conducted in four well-drained (HO1 – HO4) and four riparian plots (HOr1 – HOr4). Oil palms were planted between 1997 and 2001 in well-drained plots, and between 1998 and 2008 in riparian areas (Hennings et al., 2021), following a triangular planting scheme with ~ 9 m distance between the stems (Fig. 1a). Interrows were either used as harvesting paths or to stack cut-off palm fronds (frond pile) (Kotowska et al., 2015). In plot HO1, every interrow contained frond piles. Thus, topsoil samples of interrows were obtained only from three well-drained plots. The understory vegetation of all well-drained plots was occasionally weeded. Two riparian plots (HOr1 and HOr2) had a well-maintained grass cover between the oil palms.

In each of the eight plots, topsoil samples were taken with steel cylinders (height = 4 cm, volume = 100 cm³) at five locations along the slope. At each location, topsoils were sampled from four different management zones, *i.e.*, (1) palm circle, (2) oil-palm row, (3) interrow, and (4) frond pile, to assess spatial patterns of Si_{Am} and Si_M concentrations in topsoils within the oil-palm plantations (Appendix, Table A1 and A2). Interrow topsoil samples were taken at a maximum distance between oil palms. The samples were dried (40 °C, 24 h) and sieved ($\leq$ 2 mm) prior to Si analyses. An aliquot of each sample was dried at 105 °C to determine the water content of the samples dried at 40 °C.

2.2.2 Sediment traps

Sediment traps were installed in sets of two in interrows of the well-drained plots HO1 – HO4, on 8 – 12° sloping land (Sinukaban et al., 2000). Each trap consisted of a rectangular aluminium frame (2 x 1 m, 2 m²). Its downslope-facing short side was funnel-shaped, directing surface runoff and eroded soil material into a bucket (Fig. 1b and Appendix, Table A3). A second bucket was connected to the first bucket by a 2 cm thick tube to catch potential overflow. The traps were checked and maintained weekly from the beginning of September 2018 to the end of August 2019. The understory vegetation in the sediment traps was kept in place to ensure that the understory vegetation was representative of the oil-palm plantations. Both sediment traps in HO1 were manually weeded after six months because inside the traps, vegetation covered nearly 100 % of the soil surface, impeding topsoil erosion. Eroded soil material was collected whenever present, dried (40 °C, 48 h), sieved ($\leq$ 2 mm) and weighed prior to Si analyses. Samples of eroded soil material from plot HO2 were excluded from further analysis because both traps got contaminated by crude oil. Losses of Si_{Am} were calculated for each sediment trap by multiplying the concentration of Si_{Am} of each sediment sample by the amount of eroded soil material collected by each trap

(Appendix, Table B3). Erosion estimates were determined for each trap by summing up the amount of eroded soil material for the 12-months period from the beginning of September 2018 until the end of August 2019. Precipitation data of the two closest meteorological stations were used for correlating the observed soil erosion with precipitation. Distances between meteorological stations and plots comprised ~ 2 km for HO1, ~ 3 km for HO2, ~ 8 km for HO3, and ~ 6 km for HO4. At each meteorological station, precipitation was measured by two automated precipitation transmitters (Thies Clima, Göttingen, Germany), at a height of 1.5 m and a horizontal distance of about 6 m.
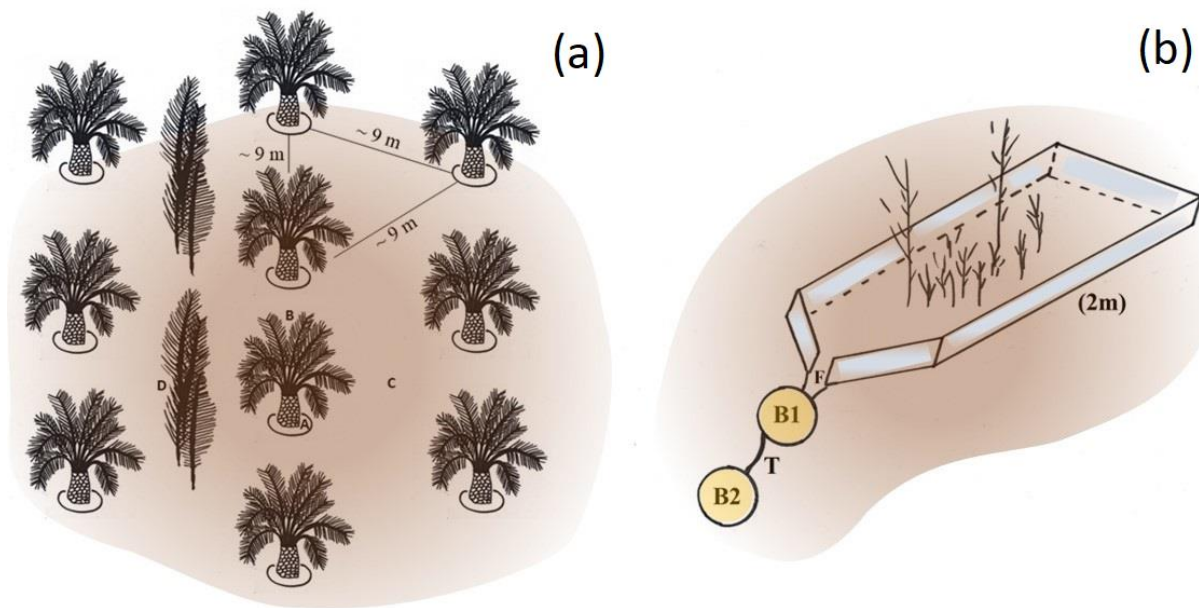
Figure 1a Triangular planting arrangement on smallholder oil-palm plantations in the study area (sketch by B. Greenshields). Topsoil samples were taken in four distinct management zones: (A) in palm circles. (B) in oil-palm rows, (C) in interrows and (D) below frond piles.
Figure 1b 2 m² sediment trap with scarce understorey vegetation installed in pairs in four well-drained plots (sketch by B. Greenshields after Sinukaban et al. 2000). The downslope funnel-shaped part of the aluminium frame (F) directs surface runoff, together with eroded soil material, into a bucket (B1) that is connected to a second bucket (B2) by a 2 cm wide tube (T). Photos of the sediment traps are shown in the Appendix, Table A3.

2.3 Determination of silicon pools in topsoils

2.3.1 Silicon in amorphous silica (Si_{Am})

Si_{Am} was extracted from topsoil samples and eroded soil material by 1 % Na_2CO_3 solution (Meunier et al., 2014). At 85 °C, amorphous silica dissolves within 2 – 3 hours in 1 % Na_2CO_3 solution, thereby rapidly raising the Si concentration in solution. Once amorphous silica is completely dissolved, the release of Si to solution is only sustained by the slower dissolution of silicate minerals which follows a linear trend. Si concentration was measured four times during the linear dissolution phase. A linear equation was fitted to the data. The Si_{Am} concentration was inferred from the y-intercept of the linear regression.

In detail, 40 ml of 1 % Na_2CO_3 solution were added to approximately 30 mg of soil material. The samples were then placed into a shaking water bath at 85 °C. To ensure steady Si release from topsoils, the samples were manually shaken at time intervals of 45 min. Aliquots were taken after 3 h, 3.75 h, 4.5 h, and 5.25 h. For this

purpose, the samples were taken out of the water bath, cooled in a cold-water basin (10 min) and centrifuged (5 min, 3000 *rpm*). A 0.25 ml aliquot was taken from the supernatant of each sample and neutralized with 2.25 ml 0.021 M HCl. Si concentrations in the aliquots were analysed by the molybdenum blue method (Grasshoff et al., 2009) using a UV-VIS spectrophotometer (Lamda 40, Perkin Elmer, Germany) at 810 nm. We chose 1 % Na_2CO_3 as an extractant and used the extraction method by Meunier et al. (2014) instead of the stronger extractant 0.1 M NaOH used by Barão et al. (2015) because we assumed that most Si in topsoils is of biogenic origin and dissolved well by Na_2CO_3 (Meunier et al., 2014).

2.3.2 Mobile silicon (Si_M)

Si_M was extracted by $CaCl_2$ solution, which provides electrolytes resembling natural soil solutions (Sauer et al., 2006; Georgiadis et al., 2013). From each sample, 1 g of soil material was mixed with 5 ml of 0.01 M $CaCl_2$ and left for 24 h, shaking for 1 min h^{-1} on an overhead shaker. Samples were centrifuged (5 min, 3000 *rpm*) and the supernatant was filtered through ash-free paper filters (1-2 µm). Si concentrations were analysed in filtrates by the molybdenum blue method. We transformed the measured Si concentration (µg g^{-1}) into the amount of Si_M per gram 105 °C dried soil.

2.4 Statistical analyses

Statistical analyses were conducted on the grand means of topsoil Si concentrations in each water regime and management zone. The two latter were grouped into (i) palm circles in well-drained / riparian areas (each, n = 4), (ii) oil-palm rows in well-drained / riparian areas (each, n = 4), (iii) interrows in well-drained (n = 3) / riparian areas (n = 4) and (iv) frond piles in well-drained / riparian areas (each, n = 4). The four management zones were tested for significant differences in topsoil Si concentrations, both within the well-drained and within the riparian areas. In addition, we tested the well-drained and riparian areas for significant differences in topsoil Si concentrations by comparing the same management zone under two different water regimes. The data was log transformed to assert normal distribution (Shapiro-Wilk test) and homogeneity of variances (Levene test). Both criteria were met for all groups except for Si_M in topsoils of oil-palm rows in well-drained areas (Appendix, Table B4). We conducted a one-way analysis of variance (ANOVA) to detect if Si_{Am} and Si_M concentrations in topsoils of different management zones differed significantly within well-drained and within riparian areas, as well as between well-drained and riparian areas. Then we used the Tuckey-Kramer post-hoc test to identify, which management zones differed significantly. The level of significance was set at $p \leq 0.05$. We used the open-source software R version 3.6.2 and R CRAN packages ggplot2 (Wickham, 2016), ggpubr (Kassambara, 2022), car (Fox and Weisberg, 2019) and psych (Revelle, 2022) to perform these statistical analyses.

3 Results

3.1 Concentrations of Si_{Am} and Si_M in topsoils

In well-drained plots, mean topsoil Si_{Am} concentrations were about twice as high under frond piles (3.97 ± 0.76 mg g^{-1}) compared to palm circles (1.71 ± 0.36 mg g^{-1}), oil-palm rows (1.87 ± 0.28 mg g^{-1}) and interrows (1.88 ± 0.32 mg g^{-1}) (Fig. 2a, Appendix Table B1). This difference between frond piles and the other three management zones was significant ($p \leq 0.05$) (Fig. 2a). In riparian plots, mean topsoil Si_{Am} concentrations were equally high below frond piles (2.96 ± 0.36 mg g^{-1}) and in interrows (2.71 ± 0.13 mg g^{-1}) (Fig. 2b). Compared to these two management zones, mean topsoil Si_{Am} concentrations in palm circles (1.44 ± 0.30 mg g^{-1}) were significantly lower ($p \leq 0.05$) (Fig. 2b). Oil-palm rows had intermediate mean topsoil Si_{Am} concentrations (2.08 ± 0.63 mg g^{-1}) (Fig. 2b), showing no significant difference with respect to any other management zone ($p \leq 0.05$).

In well-drained plots, mean topsoil Si_M concentrations were about twice as high under frond piles (13.68 ± 6.54 µg g^{-1}) and in palm circles (11.17 ± 5.42 µg g^{-1}) compared to oil-palm rows (6.38 ± 2.85 µg g^{-1}) and interrows (5.62 ± 0.10 µg g^{-1}) (Fig. 2c). Only plot HO1 showed exceptionally high topsoil Si_M concentrations in oil-palm rows (outlier), which could be attributed to the dense vegetation throughout that smallholder plantation. In riparian plots, mean topsoil Si_M concentrations were twice as high under frond piles (19.56 ± 6.13 µg g^{-1}) compared to mean topsoil Si_M concentrations in palm circles, oil-palm rows and interrows, the latter all ranging around 11 µg g^{-1} (Fig. 2d). Mean topsoil Si_M concentrations did not differ significantly ($p \leq 0.05$) between the other management zones within the same water regime (well-drained/riparian), nor did mean topsoil Si_M concentrations (in the same management zone) differ between water regimes.
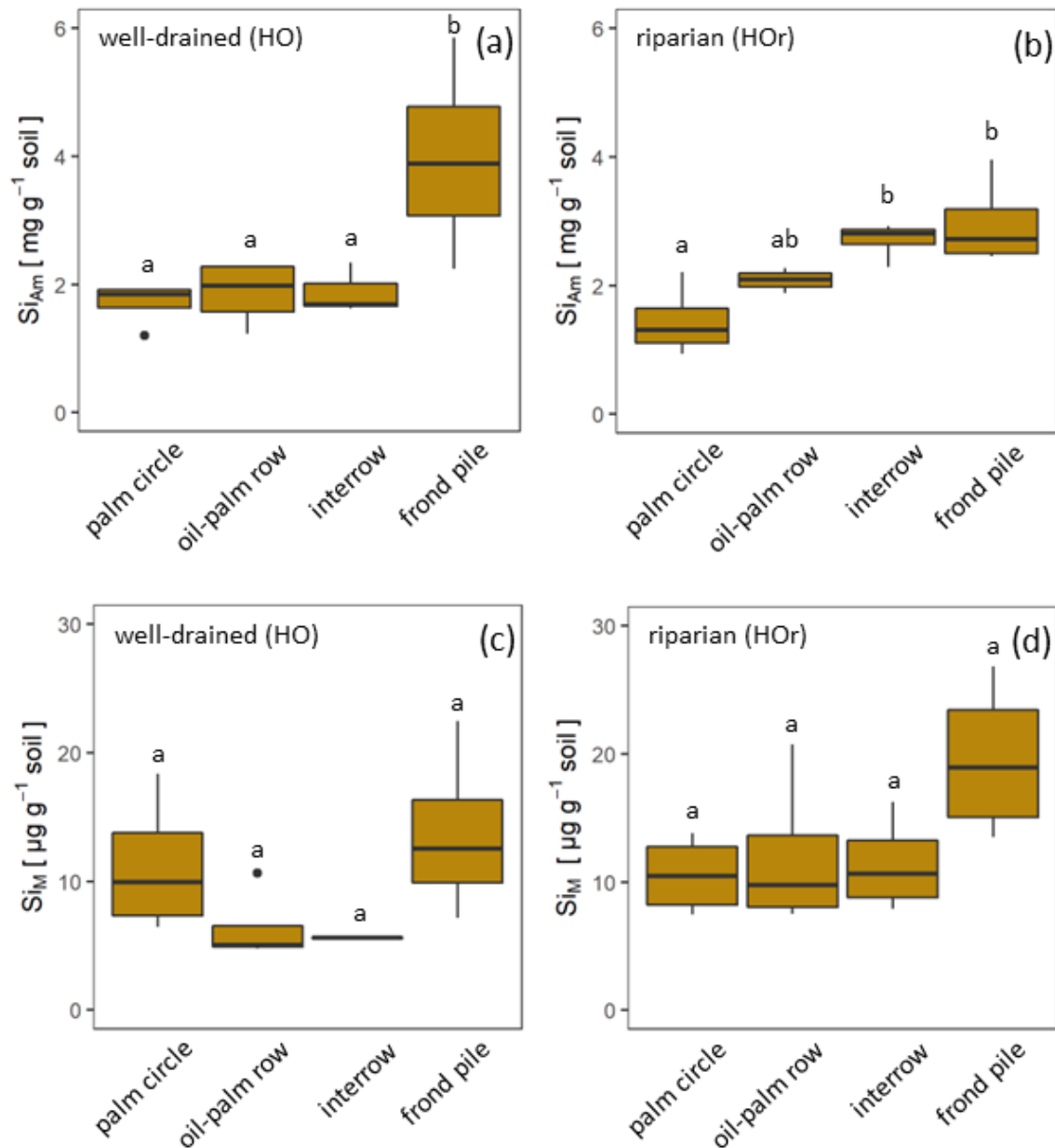
Figure 2 Concentrations of mobile Si (Si_M) and Si in amorphous silica (Si_{Am}) in topsoils of four different management zones: palm circles (n = 4), oil-palm rows (n = 4), interrows (n = 3), and under frond piles (n = 4) on smallholder oil-palm plantations in two different landscape positions with differing water regimes (well-drained and riparian). Boxes indicate interquartile ranges and whiskers extend 1.5 times the interquartile range below or above the box. If lower case letters (a, b) differ from one another, this indicates a significant difference between management zones within a water regime ($p \leq 0.05$). Si concentrations were calculated with one-way analysis of variance (ANOVA) and Tukey-Kramer post-hoc test.

3.2 Topsoil erosion and associated losses of Si_{Am}

In plots HO3 and HO4, median Si_{Am} concentrations in topsoils of interrows (1.53 – 1.57 mg g^{-1}) were roughly twice as high as in eroded soil material (0.66 – 0.88 mg g^{-1}) (Tab. 1). In plot HO1, the median Si_{Am} concentration in eroded soil material (1.61 mg g^{-1}) was twice as high as in eroded soil material of plots HO3 and HO4 (0.66 – 0.88 mg g^{-1}). Over the entire sampling period of 12 months, the four sediment traps in plots HO1 and HO4 indicated erosion rates of ~ 4 – 5 Mg ha^{-1} yr^{-1} (Tab. 2). In plot HO3, a similar erosion rate was obtained from trap 1 (~ 6 Mg

ha^{-1} yr^{-1}), whereas the erosion rate observed in trap 2 of plot HO3 was twice as high (~ 12 Mg ha^{-1} yr^{-1}). Si$_{Am}$ losses through topsoil erosion amounted to 6 – 9 kg ha^{-1} yr^{-1} in the four sediment traps of HO1 and HO3, and 5 – 7 kg ha^{-1}yr^{-1} in both sediment traps of HO4. Figure 3 presents weekly losses of topsoil and Si$_{Am}$ in eroded topsoil correlated with daily rainfalls. During the 12-month sampling period, daily rainfalls ≥ 25 mm d^{-1} were recorded from mid-September 2018 until mid-June 2019 (Fig. 3). The rainy season started in November 2018 with daily rainfalls exceeding 60 mm d^{-1} (HO4, weather station near a state-owned plantation) to 70 mm d^{-1} (HO1 and HO3, weather station near the village of Bungku) after a dry spell in October. A second rainy peak lasted from mid-March to mid-April 2019 with daily rainfalls reaching 50 mm d^{-1} (HO1 and HO3) to 70 mm d^{-1} (HO4). The dry season started in mid-June 2019, showing only one intense rainfall event (outlier, HO4) at the end of August 2019.

In plot HO1, a dense cover of mosses, grasses, and 20 – 50 cm high understorey vegetation prevented soil loss from September 2018 until end of January 2019. (Tab. 1, Fig. 3a). After manually weeding plot HO1 at the end of January 2019, the vegetation coverage was kept minimal (around 5 %). Noticeable losses of soil and corresponding losses of Si$_{Am}$ occurred between February (13 – 21 g m^{-2} of sediment, 16 – 53 mg m^{-2} of Si$_{Am}$) and the end of May 2019 (16 – 100 g m^{-2} of sediment / 38 – 192 mg m^{-2} of Si$_{Am}$) (Fig. 3a and 3b). In plot HO3, scare understorey vegetation of herbaceous plants (no grasses and mosses) covered about a third of the sediment traps (Tab. 1). Soil and corresponding Si$_{Am}$ losses were recorded continuously from September 2018 to May 2019 (Fig. 3.3). Each week, losses of topsoil material amounted to 4 – 62 g m^{-2} (corresponding to 1 – 90 mg m^{-2} Si$_{Am}$) (Fig. 3a, 3b). At three sampling dates, one in December 2018 and two in February 2019, peak soil losses ≥ 150 g m^{-2} occurred. The corresponding Si$_{Am}$ losses of these sampling dates were ≥ 90 mg m^{-2}, hence also representing among the highest Si$_{Am}$ losses throughout the sampling period. In plot HO4, vegetation coverage in the traps increased from 40 % in September 2018 to 60 % in May 2019 (Tab. 1). Soil loss occurred from mid-September 2018 to the end of May 2019 (Fig. 3). Losses of eroded soil material barely exceeded 50 g m^{-2} of sediment. However, an event with approximately 20 g m^{-2} of soil loss had corresponding Si$_{Am}$ losses ranging from 5 – 160 mg m^{-2}, thus showing a large variability.

Table 1 Topsoil Si_{Am} concentrations in interrow and sediment trap samples

Oil-palm plot	N^c	Statistics	Interrow Si_{Am} [mg g^{-1}$_{soil}$]	Eroded soil material Si_{Am} [mg g^{-1}$_{soil}$]	Estimated vegetation cover (Sep / Jan / Apr-May [%])
HO1[a]	NA/19	MIN	NA[d]	0.90	100 / 5 / 5
HO1[a]	NA/19	MEDIAN	NA[d]	**1.61**	
HO1[a]	NA/19	MEAN	NA[d]	1.77	
HO1[a]	NA/19	MAX	NA[d]	3.26	
HO3[b]	5/38	MIN	1.40	0.11	30 / 40 / 30
HO3[b]	5/38	MEDIAN	**1.53**	**0.88**	
HO3[b]	5/38	MEAN	1.63	0.82	
HO3[b]	5/38	MAX	1.91	1.97	
HO4[b]	5/27	MIN	1.45	0.03	40 / 50 / 60
HO4[b]	5/27	MEDIAN	**1.57**	**0.66**	
HO4[b]	5/27	MEAN	1.69	1.13	
HO4[b]	5/27	MAX	2.21	6.84	

[a]Si_{Am} concentrations for plot HO1 as of February 2019 (after manual weeding)
[b]Si_{Am} concentrations for plot HO3 and HO4 for the whole sampling duration
[c]replicates for interrow topsoil samples/replicates for eroded soil samples
[d]every interrow on plot HO1 contained stacked frond piles, no sampling possible

Table 2 Annual losses of soil and Si_{Am} through erosion

Plot	Trap	Eroded soil material [Mg soil ha^{-1} yr^{-1}]	Si_{Am} [kg Si_{Am} ha^{-1} yr^{-1}]
HO1	1	5.4	8.7
HO1	2	4.2	7.2
HO3	1	11.7	8.9
HO3	2	6.1	6.0
HO4	1	5.4	6.7
HO4	2	3.6	4.6

255
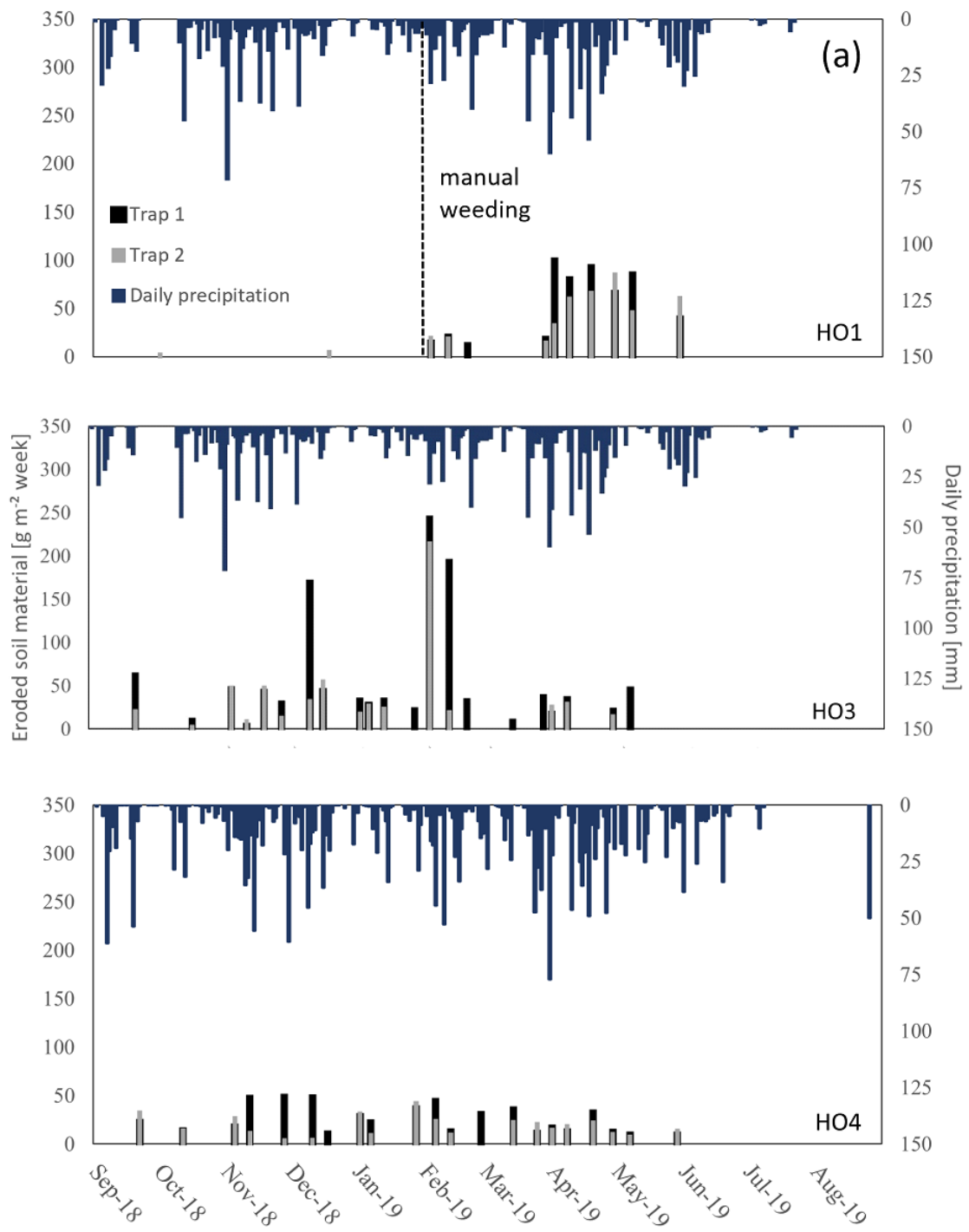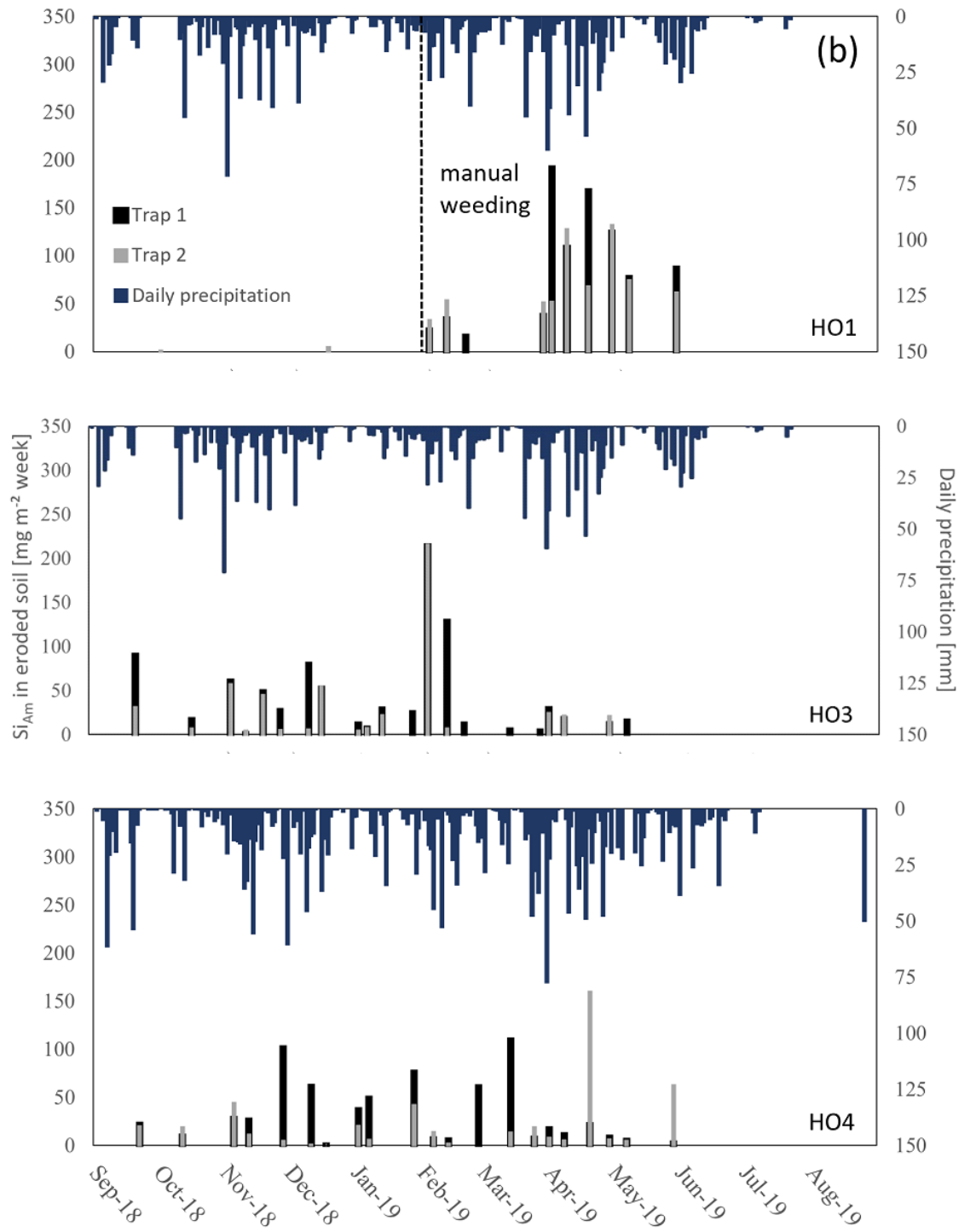
Figure 3 Weekly losses of topsoil (a) and Si in amorphous silica (Si_{Am}) in eroded topsoil (b), collected from sediment traps (n = 6) of oil-palm plantations in well-drained areas.

4 Discussion

4.1 Spatial topsoil Si_{Am} concentration patterns

In oil-palm plantations, cut-off palm fronds stacked in every second interrow represent the main source of phytoliths (Albert et al., 2015; Clymans et al., 2015; Huisman et al., 2018) although these frond pile areas may occupy less than 15 % of plantation area (Tarigan et al., 2020). Once phytoliths are released into topsoils, they can replenish the topsoil Si_{Am} pool. Therefore, we had hypothesized that Si_{Am} is mainly returned to soils under frond piles (cf. section 1), leading to a spatial topsoil Si_{Am} pattern with higher Si_{Am} concentrations under frond piles. This hypothesis was corroborated for well-drained plots as topsoil Si_{Am} concentrations were indeed significantly higher (2-fold) under frond piles (~4 mg g^{-1}) than in all other management zones (~2 mg g^{-1}) (Fig. 2a, Appendix Table B2.1). Lower Si_{Am} levels in palm circles, oil-palm rows and interrows may reflect the pedogenic Si_{Am} pool with only minor contributions of biogenic Si_{Am}, *e.g.*, from grass phytoliths. A possible reason for this is that decaying palm fronds are not returned to these management zones.

In the riparian plots, topsoil Si_{Am} concentrations were equally high under frond piles and in interrows (~ 3 mg g^{-1}). This can only be explained by an additional important source of topsoil Si_{Am} in interrows that was present in the riparian plots. The only potential Si_{Am} source includes litter of grasses (*Poaceae*) and sedges (*Cyperaceae*) which also releases considerable amounts of phytoliths upon its decomposition. Grasses and sedges are considered effective Si accumulators, too (Blecker et al., 2006; Quigley et al., 2017). This explanation is further supported by the significantly lower ($p \leq 0.05$) topsoil Si_{Am} concentrations in palm circles (~1.4 mg g^{-1}) (Fig. 2b, Appendix Table B2.2). Palm circles are weeded and treated with herbicides regularly. Thus, this management zone also lacks litter return and with that a principal source of Si. The significant difference in topsoil Si_{Am} concentrations between interrows and palm circles can only be explained by the presence or absence of grasses as phytolith sources. This observation highlights the importance of grasses and sedges in oil-palm plantations as they can also maintain soil-plant-Si cycling in the system. Thus, our original hypothesis that Si_{Am} is mainly returned to the soils under frond piles, while topsoils in other management zones tend to be depleted in Si_{Am}, is valid only in oil-palm plantations with a negligible grass cover.

The absence of any significant differences in topsoil Si_{Am} concentrations between the two differing water regimes suggests that there was no noticeable Si supply by stream water to topsoils in riparian areas. In fact, release rates of biogenic Si_{Am} from decaying oil-palm and other litter must be similar in both water regimes, likewise, the rate at which oil palms take up Si from soil solution and form phytoliths. This result contrasts with vander Linden and Delvaux (2019) and Georgiadis et al. (2017), who found soil type and soil properties to affect Si cycling, when comparing well-drained and floodplain soils: vander Linden and Delvaux (2019) observed that flooding can temporarily increase the soil pH of acidic soils to ~6.5 – 7.2. In this pH range, phytoliths dissolve faster (vander Linden and Delvaux, 2019). Georgiadis et al. (2017) pointed to the effect of alternating redox conditions in soils as caused *e.g.*, by perched water, a fluctuating groundwater table and flooding. When pedogenic Fe, Al or Mn oxides and hydroxides are exposed to reducing conditions during flooding, they dissolve and release occluded Si into soil solution. After flooding, when the soil is exposed to oxidizing conditions again, Si can be occluded in and adsorbed to the surfaces of newly formed pedogenic oxides and hydroxides (Georgiadis et al., 2017). Georgiadis et al. (2017) found that these redox-induced dynamics affected mainly the following Si fractions: Si in soil solution (mobile Si), Si adsorbed to, and Si occluded in Fe oxides and hydroxides. Many other researchers found soil pH,

soil texture and soil chemistry to govern biogenic and pedogenic Si pools down to at least 1 m soil depth (Alexandre et al., 1997; Struyf and Conley, 2009; Li et al., 2020). The latter soil characteristics were kept constant in our study as we focused specifically on the effect of flooding. The reason that we did not detect any effect of flooding might be the advanced weathering and desilication status of the soils in our study area, which may have led to overall low Si levels of the investigated soils.

4.2 Si_{Am} losses through topsoil erosion

Corley and Tinker (2016) summarized some early works by Kee and Chew (1996) and Maene et al. (1979) estimating soil-erosion rates under oil-palm plantations. They reported losses of ≤ 9 Mg ha^{-1} yr^{-1} from sloping oil-palm plantations on Plinthic Acrisols and Haplic Nitisols in Malaysia (Arshad, 2015; Corley and Tinker, 2016). In our study we obtained soil losses of ~ 4 – 6 Mg ha^{-1} yr^{-1}. This puts our estimates into a comparable range (except for trap 1 in plot HO3 that yielded ~ 12 Mg ha^{-1} yr^{-1}). However, short-term experiments can easily overestimate soil erosion rates, if upscaled to landscape level (Breuning-Madsen et al., 2017). The observations by Breuning-Madsen et al. (2017) would imply that the soil losses we obtained for oil-palm plantations are ~ 2 orders of magnitude higher than in a secondary forest (Breuning-Madsen et al., 2017). Considerable erosion (soil loss of ~ 35 cm during a 15-year cultivation period, which corresponds to ~ 28 Mg ha^{-1} yr^{-1}) was noted by Guillaume et al. (2015), who compared $\delta^{13}C$ values in soil profiles on the same well-drained oil-palm plantations of our study region. High erosion rates are to be expected, as oil-palm plantations have a rather open canopy compared to rainforests, permitting rain drops to directly hit the ground (Oliveira et al., 2013; Corley and Tinker, 2016).

During heavy rainfalls, rain drops release kinetic energy that breaks up soil aggregates, especially when hitting bare soil. Mobilized fine and broken aggregates can fill soil pores thereby reducing infiltration, promoting surface run-off (Oliveira et al., 2013; Tarigan et al., 2020) and hence erosion. Besides, soil compaction may be substantial in oil-palm interrows, which are frequently used as harvesting paths and are therefore kept vegetation-free, which makes them particularly prone to surface runoff and erosion (Comte et al., 2012; Guillaume et al., 2016). This explanation is further supported by our sediment trap data: traps with a low vegetation cover (*e.g.*, HO3 whole year and HO1 as of February 2019) exposed to daily rainfalls exceeding 25 mm d^{-1} showed higher losses of soil (~ 50 – 100 g m^{-2}, Tab 1. and Fig. 3a) than traps (*e.g.*, HO4 whole year and HO1 prior to February 2019) that had less than 50 % of bare soil at similar rainfall intensities. This again highlights the importance of cover crop in oil-palm plantations countering soil erosion (Guillaume et al., 2016, 2015; Corley and Tinker, 2016; Luke et al., 2019). Furthermore, stacked palm fronds, especially if aligned perpendicular to the slope, may reduce soil erosion on oil-palm plantations (Corley and Tinker, 2016).

One of the questions to be answered in this study was, to what extent soil erosion reduces the topsoil Si_{Am} pool in oil-palm plantations, and whether the lower density of phytoliths compared to mineral soil particles caused proportionally greater losses of Si_{Am} through soil erosion. To our knowledge, only a few studies exist, in which the effect of soil erosion on the topsoil Si_{Am} pool has been addressed. Almost all of them focused on arable soils (Clymans et al., 2015; Unzué-Belmonte et al., 2017; Kraushaar et al., 2021). Clymans et al. (2015) determined mean topsoil Si_{Am} concentrations of 1.76 mg^{-1} g^{-1} in arable fields in sloping terrain and temperate climate. This compares well to topsoil Si_{Am} concentrations in interrows from our study (Tab. 1). In contrast, Si_{Am} concentrations in eroded soil material differed by factor two between plots HO1 (1.61 mg g^{-1}) towards HO3 (0.88 mg g^{-1}) and HO4 (0.66 mg g^{-1}) (Tab. 1 and Appendix, Table B3). A possible explanation could be the differing maintenance

of the cover crop. High median Si_{Am} concentrations in eroded soil material were determined in previously vegetated traps (*e.g.*, HO1 until the end of January 2019), whereas lower median Si_{Am} concentrations in eroded soil material were measured in traps with less vegetation (HO3 and HO4, whole year, Tab. 1). We may infer from this observation that the cover crop in plot HO1 maintained higher Si levels in the topsoil through continuous phytolith release from litter. After weeding and keeping the vegetation cover at around 5 %, this phytolith-enriched topsoil was eroded leading to higher Si_{Am} concentrations in the eroded soil material. In contrast, plots HO3 and HO4 had lower, and more dispersed Si_{Am} concentrations in eroded soil material as they lacked an additional Si source. Further, low Si_{Am} concentrations suggest that topsoil with originally high amounts of biogenic Si_{Am} has already been eroded over time, leaving mainly pedogenic Si_{Am}. A greater variability in Si_{Am} concentrations in eroded soil material in plots HO3 and HO4 was probably caused by a slight increase in vegetation cover during the year and secondarily, by varying daily rainfalls (Fig. 3). Thus, these observations could provide a basis to state that phytoliths are preferably eroded from topsoils. This in turn would assert our hypothesis. Nevertheless, further field experiments and observations are required to confirm this statement.

4.3 Spatial topsoil Si_M concentration patterns

Topsoil Si_M concentrations in well-drained plots were highest under frond piles (~14 µg g^{-1}), followed by palm circles (~11 µg g^{-1}), and lowest in oil-palm rows and interrows (~6 µg g^{-1}). However, these differences were not statistically significant (Fig. 2c, 2d). Higher topsoil Si_M concentrations under frond piles can be explained by the high solubility of Si_{Am} that is released from decaying palm fronds in the form of phytoliths. In addition to Si_{Am} (Barão et al., 2014; Unzué-Belmonte et al., 2017), Si associated to soil organic matter (SOM) also represents a readily soluble Si fraction in topsoils (Alexandre et al., 1997; Georgiadis et al., 2013; von der Lühe et al., 2020). Such readily soluble Si fractions usually contribute most Si to soil solution (Struyf et al., 2010; de Tombeur et al., 2020).

The plots in the riparian areas showed high topsoil Si_M concentrations under the frond piles (~20 µg g^{-1}). All other management zones had lower topsoil Si_M concentrations in the range of ~11 – 12 µg g^{-1} (Fig. 2b). However, this difference was also not statistically significant. In riparian plots, flooding may lead to a redistribution of Si_M across the oil-palm plantation, hence explaining similar topsoil Si_M concentrations in palm circles, oil-palm rows and interrows. In riparian areas that are flooded during the rainy season, dissolved Si in stream water (Cornelis et al., 2011; Dürr et al., 2011) may be another source of topsoil Si_M alongside Si_{Am}. Therefore, we had hypothesised that Si input from stream water may lead to higher topsoil Si_M levels in riparian areas compared to well-drained areas. Indeed, topsoil Si_M concentrations under frond piles in riparian plots (~20 µg g^{-1}) tended to be higher compared to well-drained plots (~14 µg g^{-1}). Likewise, topsoil Si_M concentrations in oil-palm rows and interrows in riparian plots (~11-12 µg g^{-1}) also tended to be higher compared to well-drained plots (~6 µg g^{-1}). However, these differences were not statistically significant so our hypothesis cannot be fully asserted.

5 Conclusions and recommended measures

Based on the differing topsoil Si_{Am} concentrations observed in the different management zones, we conclude that current oil-palm management practices cause a distinct spatial topsoil Si_{Am} concentration pattern. Especially the stacking of cut-off palm fronds in long piles and subsequent decomposition promotes Si_{Am} return to soils. Thus, highest topsoil Si_{Am} concentrations occur below frond piles. Similarly, high concentrations may be found in

interrows, if additional sources of biogenic Si_{Am} such as Si-accumulating plants (grasses, sedges) are present. Lower topsoil Si_{Am} concentrations in oil-palm rows and unvegetated interrows reflect a lack of Si_{Am} return to soils through plant litter in these management zones. Moreover, pronounced topsoil erosion in unvegetated interrows involves Si_{Am} losses and may therefore cause additional Si_{Am} depletion in this management zone. A dense cover of grasses and mosses in interrows may efficiently reduce erosion and associated Si_{Am} losses.

Topsoil Si_M concentrations in the different management zones showed that biogenic Si_{Am} was an important readily available source of Si_M. Thus, analogous to topsoil Si_{Am} concentrations, highest topsoil Si_M concentrations also occurred under frond piles. Our hypothesis that regular flooding involves an input of Si dissolved in stream water into the system in riparian areas, partially replenishing the Si_M pool, could not be statistically proven in this study. Although topsoil Si_M concentrations tended to be higher in riparian areas, the differences between well-drained and riparian plots were not statistically significant.

In conclusion, our findings suggest that erosion could be reduced efficiently, and Si cycling could be maintained within the system if smallholders followed some suggested measures such as (1) maintaining a grass cover in oil-palm rows and interrows, (2), incorporating oil-palm litter into plantation management and (3) preventing soil compaction and surface-crust formation. It would be advisable to raise awareness on topsoil erosion and its potential causes. Furthermore, any logistical efforts and costs involved for implementing these measures (*e.g.*, for ameliorating soil compaction) would have to be feasible.

6 Appendix

Table A1 Representative elevation transects of topsoil sampling under oil-palm plantations

Plot	GPS position 1		GPS position 2		Elevation [m]
HO1	S 01° 54.583'	E 103° 15.996'	S 01° 54.587'	E 103° 16.015'	85
HO2	S 01° 53.012'	E 103° 16.017'	S 01° 52.987'	E 103° 16.018'	76
HO3	S 01° 51.442'	E 103° 18.490'	S 01° 51.445'	E 103° 18.522'	25
HO4	S 01° 47.188'	E 103° 16.246'	S 01° 47.195'	E 103° 16.229'	60
HOr1	S 01° 54.107'	E 103° 22.887'	S 01° 54.124'	E 103° 22.993'	28
HOr2	***	***	***	***	***
HOr3	S 01° 51.662'	E 103° 18.357'	S 01° 51.656'	E 103° 18.383'	48
HOr4	S 01° 42.687'	E 103° 17.544'	S 01° 42.666'	E 103° 17.536'	33

395

Table A2 Topsoil sampling, fieldwork 2018

HO1 – oil-palm row	HO1 – oil-palm row (detailed view)

Table A3 Sediment traps in interrows of well-drained oil-palm plantations.

HO1 – September 2018	HO1 – February 2019	HO1 – May 2019
HO3 – September 2018	HO3 – January 2019	HO3 – April 2019
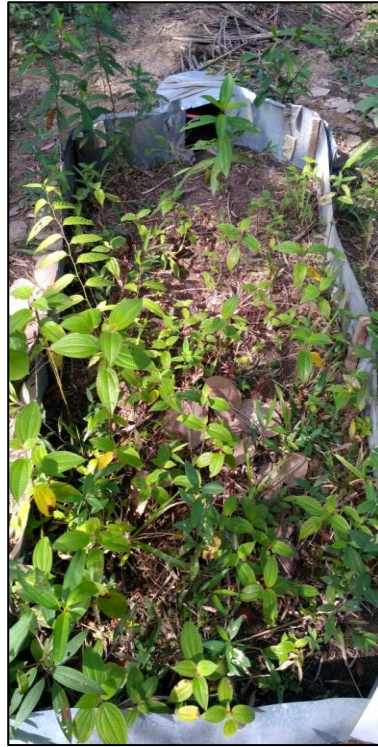
| HO4 – September 2018 | HO4 – January 2019 | HO4 – May 2019 |

| Well-drained – Interrow | Riparian – Interrow |

400

Table B1 Mean topsoil Si concentrations in different management zones of oil-palm plantations

Management zone	Plot	Water regime	Si_{Am} [mg g^{-1}$_{soil}$] $\bar{x}$	σ	Si_{M} [µg g^{-1}$_{soil}$] $\bar{x}$	σ
Palm circle	HO1	Well-drained	1.93 ±	0.25	12.23 ±	4.83
Palm circle	HO2	Well-drained	1.92 ±	0.70	7.61 ±	4.13
Palm circle	HO3	Well-drained	1.78 ±	1.08	18.38 ±	5.47
Palm circle	HO4	Well-drained	1.20 ±	0.43	6.45 ±	3.10
Oil-palm row	HO1	Well-drained	2.27 ±	0.93	10.65 ±	1.96
Oil-palm row	HO2	Well-drained	2.28 ±	0.31	5.17 ±	1.15
Oil-palm row	HO3	Well-drained	1.23 ±	0.54	4.77 ±	0.49
Oil-palm row	HO4	Well-drained	1.68 ±	0.35	4.94 ±	0.83
Interrow	HO1	Well-drained	*** ±		*** ±	
Interrow	HO2	Well-drained	2.34 ±	0.81	5.52 ±	1.16
Interrow	HO3	Well-drained	1.63 ±	0.21	5.72 ±	1.56
Interrow	HO4	Well-drained	1.69 ±	0.30	5.64 ±	2.39
Frond pile	HO1	Well-drained	4.42 ±	1.47	22.47 ±	10.7
Frond pile	HO2	Well-drained	5.86 ±	2.25	10.81 ±	2.37
Frond pile	HO3	Well-drained	3.35 ±	0.92	14.26 ±	4.03
Frond pile	HO4	Well-drained	2.24 ±	0.50	7.18 ±	1.50
Palm circle	HOr1	Riparian	0.94 ±	1.02	8.46 ±	2.54
Palm circle	HOr2	Riparian	2.21 ±	0.62	12.44 ±	1.55
Palm circle	HOr3	Riparian	1.46 ±	0.46	7.49 ±	2.34
Palm circle	HOr4	Riparian	1.16 ±	0.33	13.82 ±	1.56
Oil-palm row	HOr1	Riparian	2.27 ±	1.62	8.23 ±	4.78
Oil-palm row	HOr2	Riparian	2.02 ±	0.54	20.74 ±	3.48
Oil-palm row	HOr3	Riparian	1.88 ±	0.20	7.50 ±	0.97
Oil-palm row	HOr4	Riparian	2.17 ±	0.42	11.30 ±	0.42
Interrow	HOr1	Riparian	2.29 ±	0.64	9.07 ±	2.67
Interrow	HOr2	Riparian	2.86 ±	0.69	16.26 ±	2.50
Interrow	HOr3	Riparian	2.76 ±	0.46	7.92 ±	1.03
Interrow	HOr4	Riparian	2.93 ±	0.76	12.26 ±	2.49
Frond pile	HOr1	Riparian	2.51 ±	0.81	13.53 ±	4.70
Frond pile	HOr2	Riparian	2.46 ±	1.51	26.83 ±	2.71
Frond pile	HOr3	Riparian	3.95 ±	1.24	15.57 ±	4.63
Frond pile	HOr4	Riparian	2.93 ±	0.77	22.30 ±	11.1

Table B2.1 Topsoil Si concentrations in different management zones of well-drained oil-palm plantations

Management zone	Plot	Si_{Am} [mg g^{-1}$_{soil}$]			Si_M [µg g^{-1}$_{soil}$]		
		x	$\bar{x}$ (plot)	σ (plot)	x	$\bar{x}$ (plot)	σ (plot)
Palm circle 1	HO1	1.77	1.93 ± 0.25		12.04	12.23 ± 4.83	
Palm circle 2	HO1	2.33			10.26		
Palm circle 3	HO1	1.98			8.51		
Palm circle 4	HO1	1.68			20.57		
Palm circle 5	HO1	1.89			9.78		
Palm circle 1	HO2	2.53	1.92 ± 0.70		5.36	7.61 ± 4.13	
Palm circle 2	HO2	2.70			9.59		
Palm circle 3	HO2	1.87			3.46		
Palm circle 4	HO2	1.43			13.85		
Palm circle 5	HO2	1.06			5.80		
Palm circle 1	HO3	0.85	1.78 ± 1.08		14.52	18.38 ± 5.47	
Palm circle 2	HO3	0.86			13.45		
Palm circle 3	HO3	1.66			15.40		
Palm circle 4	HO3	3.46			25.35		
Palm circle 5	HO3	2.09			23.18		
Palm circle 1	HO4	0.68	1.20 ± 0.43		5.24	6.45 ± 3.10	
Palm circle 2	HO4	1.77			3.51		
Palm circle 3	HO4	1.27			11.46		
Palm circle 4	HO4	0.88			7.24		
Palm circle 5	HO4	1.40			4.79		
Oil-palm row 1	HO1	2.85	2.27 ± 0.93		8.01	10.65 ± 1.96	
Oil-palm row 2	HO1	0.99			10.00		
Oil-palm row 3	HO1	2.86			10.03		
Oil-palm row 4	HO1	1.59			12.62		
Oil-palm row 5	HO1	3.09			12.59		
Oil-palm row 1	HO2	2.14	2.28 ± 0.31		6.27	5.17 ± 1.15	
Oil-palm row 2	HO2	2.78			4.79		
Oil-palm row 3	HO2	2.26			6.41		
Oil-palm row 4	HO2	1.95			3.68		
Oil-palm row 5	HO2	2.29			4.69		
Oil-palm row 1	HO3	0.35	1.23 ± 0.54		4.75	4.77 ± 0.49	
Oil-palm row 2	HO3	1.43			4.49		
Oil-palm row 3	HO3	1.57			4.45		
Oil-palm row 4	HO3	1.11			5.62		
Oil-palm row 5	HO3	1.71			4.53		
Oil-palm row 1	HO4	1.57	1.68 ± 0.35		6.15	4.94 ± 0.83	
Oil-palm row 2	HO4	1.29			4.98		
Oil-palm row 3	HO4	2.19			4.78		
Oil-palm row 4	HO4	1.88			4.96		
Oil-palm row 5	HO4	1.50			3.82		
Interrow 1	HO2	3.72	2.34 ± 0.81		7.42	5.52 ± 1.16	
Interrow 2	HO2	1.63			4.89		
Interrow 3	HO2	1.99			5.00		
Interrow 4	HO2	2.30			4.47		
Interrow 5	HO2	2.04			5.79		
Interrow 1	HO3	1.78	1.63 ± 0.21		4.50	5.72 ± 1.56	
Interrow 2	HO3	1.40			7.89		
Interrow 3	HO3	1.91			4.56		
Interrow 4	HO3	1.53			4.77		
Interrow 5	HO3	1.52			6.88		
Interrow 1	HO4	1.57	1.69 ± 0.30		9.63	5.64 ± 2.39	
Interrow 2	HO4	2.21			5.44		
Interrow 3	HO4	1.64			3.43		
Interrow 4	HO4	1.57			4.22		
Interrow 5	HO4	1.45			5.46		
Frond pile 1	HO1	6.57	4.42 ± 1.47		17.35	22.47 ± 10.66	
Frond pile 2	HO1	3.50			18.93		
Frond pile 3	HO1	4.62			28.81		
Frond pile 4	HO1	4.70			37.30		
Frond pile 5	HO1	2.69			9.98		
Frond pile 1	HO2	7.06	5.86 ± 2.25		10.06	10.81 ± 2.37	
Frond pile 2	HO2	9.05			14.79		
Frond pile 3	HO2	3.51			8.76		
Frond pile 4	HO2	5.53			9.44		
Frond pile 5	HO2	4.14			11.00		
Frond pile 1	HO3	3.26	3.35 ± 0.92		10.39	14.26 ± 4.03	
Frond pile 2	HO3	4.05			11.42		
Frond pile 3	HO3	1.84			16.07		
Frond pile 4	HO3	3.47			13.07		
Frond pile 5	HO3	4.10			20.36		
Frond pile 1	HO4	1.89	2.24 ± 0.50		7.05	7.18 ± 1.50	
Frond pile 2	HO4	2.19			6.99		
Frond pile 3	HO4	3.04			9.66		
Frond pile 4	HO4	1.77			6.63		
Frond pile 5	HO4	2.33			5.57		

405

Table B2.2 Topsoil Si concentrations in different management zones of riparian oil-palm plantations

Management zone	Plot	Si_{Am} [mg g^{-1}$_{soil}$] x	$\overline{x}$ (plot)		σ (plot)	Si_{M} [µg g^{-1}$_{soil}$] x	$\overline{x}$ (plot)		σ (plot)
Palm circle 1	HOr1	0.22	0.94	±	1.02	5.73	8.46	±	2.54
Palm circle 2	HOr1	0.09				9.66			
Palm circle 3	HOr1	2.61				12.16			
Palm circle 4	HOr1	0.66				8.05			
Palm circle 5	HOr1	1.11				6.72			
Palm circle 1	HOr2	1.76	2.21	±	0.62	13.62	12.44	±	1.55
Palm circle 2	HOr2	2.70				9.76			
Palm circle 3	HOr2	1.47				12.63			
Palm circle 4	HOr2	2.95				12.75			
Palm circle 5	HOr2	2.17				13.42			
Palm circle 1	HOr3	0.68	1.46	±	0.46	6.48	7.49	±	2.34
Palm circle 2	HOr3	1.65				10.78			
Palm circle 3	HOr3	1.48				8.70			
Palm circle 4	HOr3	1.58				6.83			
Palm circle 5	HOr3	1.91				4.64			
Palm circle 1	HOr4	1.28	1.16	±	0.33	16.24	13.82	±	1.56
Palm circle 2	HOr4	0.66				13.95			
Palm circle 3	HOr4	1.10				13.33			
Palm circle 4	HOr4	1.56				11.92			
Palm circle 5	HOr4	1.20				13.67			
Oil-palm row 1	HOr1	0.60	2.27	±	1.62	2.13	8.23	±	4.78
Oil-palm row 2	HOr1	1.87				6.57			
Oil-palm row 3	HOr1	2.40				12.14			
Oil-palm row 4	HOr1	4.91				13.94			
Oil-palm row 5	HOr1	1.59				6.39			
Oil-palm row 1	HOr2	2.03	2.02	±	0.54	19.30	20.74	±	3.48
Oil-palm row 2	HOr2	1.22				18.74			
Oil-palm row 3	HOr2	1.84				26.89			
Oil-palm row 4	HOr2	2.38				18.73			
Oil-palm row 5	HOr2	2.62				20.03			
Oil-palm row 1	HOr3	2.07	1.88	±	0.20	8.72	7.50	±	0.97
Oil-palm row 2	HOr3	1.95				7.21			
Oil-palm row 3	HOr3	1.86				8.28			
Oil-palm row 4	HOr3	1.97				6.49			
Oil-palm row 5	HOr3	1.54				6.77			
Oil-palm row 1	HOr4	1.47	2.17	±	0.42	10.90	11.30	±	0.42
Oil-palm row 2	HOr4	2.21				11.02			
Oil-palm row 3	HOr4	2.26				11.30			
Oil-palm row 4	HOr4	2.27				11.31			
Oil-palm row 5	HOr4	2.62				11.98			
Interrow 1	HOr1	1.58	2.29	±	0.64	13.47	9.07	±	2.67
Interrow 2	HOr1	2.05				6.98			
Interrow 3	HOr1	3.07				6.99			
Interrow 4	HOr1	2.84				9.43			
Interrow 5	HOr1	1.91				8.46			
Interrow 1	HOr2	3.36	2.86	±	0.69	19.01	16.26	±	2.50
Interrow 2	HOr2	3.72				16.00			
Interrow 3	HOr2	2.77				17.91			
Interrow 4	HOr2	2.39				15.96			
Interrow 5	HOr2	2.05				12.44			
Interrow 1	HOr3	2.20	2.76	±	0.46	8.08	7.92	±	1.03
Interrow 2	HOr3	2.52				6.54			
Interrow 3	HOr3	2.66				9.41			
Interrow 4	HOr3	3.43				8.02			
Interrow 5	HOr3	2.96				7.59			
Interrow 1	HOr4	3.19	2.93	±	0.76	10.46	12.26	±	2.49
Interrow 2	HOr4	1.78				10.67			
Interrow 3	HOr4	3.83				12.26			
Interrow 4	HOr4	2.68				16.53			
Interrow 5	HOr4	3.13				11.37			
Frond pile 1	HOr1	1.46	2.51	±	0.81	21.41	13.53	±	4.70
Frond pile 2	HOr1	2.14				13.01			
Frond pile 3	HOr1	2.35				8.80			
Frond pile 4	HOr1	3.49				12.27			
Frond pile 5	HOr1	3.12				12.16			
Frond pile 1	HOr2	4.51	2.46	±	1.51	25.28	26.83	±	2.71
Frond pile 2	HOr2	1.54				30.01			
Frond pile 3	HOr2	1.43				26.97			
Frond pile 4	HOr2	1.18				28.73			
Frond pile 5	HOr2	3.63				23.19			
Frond pile 1	HOr3	3.40	3.95	±	1.24	13.24	15.57	±	4.63
Frond pile 2	HOr3	3.65				14.54			
Frond pile 3	HOr3	5.43				19.07			
Frond pile 4	HOr3	4.94				21.28			
Frond pile 5	HOr3	2.34				9.69			
Frond pile 1	HOr4	2.50	2.93	±	0.77	16.99	22.30	±	11.06
Frond pile 2	HOr4	2.57				20.67			
Frond pile 3	HOr4	2.42				14.57			
Frond pile 4	HOr4	2.88				17.56			
Frond pile 5	HOr4	4.28				41.70			

Table B3 Weekly loss of eroded soil material and Si_{Am} in eroded soil material from sediments traps under oil-palm plantations (sloping terrain)

Date	Month	Trap	Plot	Si_{Am} [mg g^{-1} soil] $\bar{x}$	σ	Eroded soil material [g per 2m² trap]	Eroded soil material [g m^{-2}]	Si_{Am} in eroded soil material [mg m^{-2}]
2018-10-02	October	HO1_2	HO1	0.21 ±	0.03	5.59	2.80	0.6
2018-12-19	December	HO1_2	HO1	0.79 ±	0.07	11.67	5.84	4.6
2019-02-04	February	HO1_1	HO1	1.48 ±	0.18	30.83	15.42	22.8
2019-02-04	February	HO1_2	HO1	1.59 ±	0.07	41.10	20.55	32.6
2019-02-12	February	HO1_1	HO1	1.61 ±	0.26	42.08	21.04	34.0
2019-02-12	February	HO1_2	HO1	2.66 ±	0.29	39.92	19.96	53.1
2019-02-21	February	HO1_1	HO1	1.28 ±	0.05	25.26	12.63	16.2
2019-03-29	March	HO1_1	HO1	1.99 ±	0.04	37.83	18.92	37.6
2019-03-29	March	HO1_2	HO1	3.26 ±	0.04	31.40	15.70	51.2
2019-04-02	April	HO1_1	HO1	1.92 ±	0.11	200.29	100.15	191.8
2019-04-02	April	HO1_2	HO1	1.53 ±	0.28	67.23	33.62	51.6
2019-04-09	April	HO1_1	HO1	1.35 ±	0.02	161.75	80.88	109.0
2019-04-09	April	HO1_2	HO1	2.10 ±	0.49	121.74	60.87	127.6
2019-04-19	April	HO1_1	HO1	1.80 ±	0.23	186.72	93.36	168.0
2019-04-19	April	HO1_2	HO1	1.01 ±	0.04	134.16	67.08	68.0
2019-04-30	April	HO1_1	HO1	1.87 ±	0.24	133.01	66.51	124.4
2019-04-30	April	HO1_2	HO1	1.53 ±	0.19	172.16	86.08	131.8
2019-05-08	May	HO1_1	HO1	0.90 ±	0.12	171.75	85.88	77.6
2019-05-08	May	HO1_2	HO1	1.59 ±	0.28	93.65	46.83	74.4
2019-05-30	May	HO1_1	HO1	2.15 ±	0.08	80.67	40.34	86.9
2019-05-30	May	HO1_2	HO1	2.09 ±	0.18	122.74	61.37	128.4
2018-09-22	September	HO3_1	HO3	1.45 ±	0.24	124.31	62.16	89.8
2018-09-22	September	HO3_2	HO3	1.44 ±	0.25	42.84	21.42	30.9
2018-10-18	October	HO3_1	HO3	1.69 ±	0.22	19.95	9.98	16.9
2018-10-18	October	HO3_2	HO3	1.97 ±	0.19	6.72	3.36	6.6
2018-11-05	November	HO3_1	HO3	1.30 ±	0.11	93.32	46.66	60.6
2018-11-05	November	HO3_2	HO3	1.17 ±	0.25	97.70	48.85	57.0
2018-11-12	November	HO3_1	HO3	0.24 ±	0.04	8.36	4.18	1.0
2018-11-12	November	HO3_2	HO3	0.44	***	20.11	10.06	4.4
2018-11-20	November	HO3_1	HO3	1.12 ±	0.68	87.21	43.61	48.7
2018-11-20	November	HO3_2	HO3	0.91 ±	0.19	97.14	48.57	44.3
2018-11-28	November	HO3_1	HO3	0.92 ±	0.06	59.13	29.57	27.2
2018-11-28	November	HO3_2	HO3	0.34	***	27.89	13.94	4.7
2018-12-11	December	HO3_1	HO3	0.47 ±	0.11	339.32	169.66	80.0
2018-12-11	December	HO3_2	HO3	0.16	***	66.67	33.34	5.3
2018-12-17	December	HO3_1	HO3	1.18 ±	0.12	88.58	44.29	52.5
2018-12-17	December	HO3_2	HO3	0.97 ±	0.10	111.93	55.97	54.3
2019-01-03	January	HO3_1	HO3	0.36 ±	0.01	66.16	33.08	11.9
2019-01-03	January	HO3_2	HO3	0.25	***	36.69	18.35	4.6
2019-01-07	January	HO3_1	HO3	0.26 ±	0.07	57.58	28.79	7.6
2019-01-07	January	HO3_2	HO3	0.25	***	55.62	27.81	7.0

Date	Month	Sample	Site	Value	±	Error		Col1	Col2	Col3
2019-01-14	January	HO3_1	HO3	0.89	±	0.39		66.12	33.06	29.3
2019-01-14	January	HO3_2	HO3	0.88	±	0.18		49.11	24.56	21.6
2019-01-28	January	HO3_1	HO3	1.11	±	0.49		44.74	22.37	24.8
2019-02-04	February	HO3_1	HO3	0.88	±	0.14		487.59	243.80	214.5
2019-02-04	February	HO3_2	HO3	1.35	±	0.20		431.29	215.65	290.2
2019-02-13	February	HO3_1	HO3	0.66	±	0.06		387.81	193.91	128.3
2019-02-13	February	HO3_2	HO3	0.34	±	0.19		40.13	20.07	6.8
2019-02-21	February	HO3_1	HO3	0.37		***		65.28	32.64	12.1
2019-03-14	March	HO3_1	HO3	0.61		***		18.06	9.03	5.5
2019-03-28	March	HO3_1	HO3	0.11		***		75.35	37.68	4.1
NA	March	NA	HO3	0.96	±	0.10	NA	NA	NA	NA
2019-04-01	April	HO3_1	HO3	1.60	±	0.11		36.99	18.50	29.5
2019-04-01	April	HO3_2	HO3	0.89	±	0.14		53.63	26.82	24.0
2019-04-08	April	HO3_1	HO3	0.52	±	0.09		69.87	34.94	18.2
2019-04-08	April	HO3_2	HO3	0.72	±	0.14		59.92	29.96	21.4
2019-04-29	April	HO3_1	HO3	0.59	±	0.25		43.59	21.80	12.8
2019-04-29	April	HO3_2	HO3	1.30	±	0.07		31.80	15.90	20.6
2019-05-07	May	HO3_1	HO3	0.34	±	0.13		91.91	45.96	15.6
2018-09-22	September	HO4_1	HO4	0.93	±	0.07		47.19	23.60	22.0
2018-09-22	September	HO4_2	HO4	0.58	±	0.02		66.24	33.12	19.3
2018-10-12	October	HO4_1	HO4	0.66	±	0.07		29.13	14.57	9.7
2018-10-12	October	HO4_2	HO4	1.25	±	0.17		29.62	14.81	18.6
2018-11-05	November	HO4_1	HO4	1.49	±	0.05		37.52	18.76	28.0
2018-11-05	November	HO4_2	HO4	1.61	±	0.57		54.48	27.24	43.8
2018-11-12	November	HO4_1	HO4	0.54	±	0.00		97.00	48.50	26.3
2018-11-12	November	HO4_2	HO4	0.87	±	0.02		24.67	12.33	10.7
2018-11-28	November	HO4_1	HO4	2.05	±	0.10		98.97	49.48	101.6
2018-11-28	November	HO4_2	HO4	0.89	±	0.15		9.50	4.75	4.2
2018-12-11	December	HO4_1	HO4	1.27	±	0.09		97.17	48.58	61.5
2018-12-11	December	HO4_2	HO4	0.13	±	0.07		10.44	5.22	0.7
2018-12-18	December	HO4_1	HO4	0.03		***		22.42	11.21	0.3
2018-12-27	December	HO4_2	NA	NA		***	NA	NA	NA	NA
2019-01-02	January	HO4_1	HO4	1.29	±	0.09		58.14	29.07	37.4
2019-01-02	January	HO4_2	HO4	0.63	±	0.17		64.15	32.08	20.3
2019-01-07	January	HO4_1	HO4	2.15	±	0.03		45.88	22.94	49.3
2019-01-07	January	HO4_2	HO4	0.56	±	0.13		19.82	9.91	5.6
2019-01-28	January	HO4_1	HO4	2.03	±	0.06		75.12	37.56	76.2
2019-01-28	January	HO4_2	HO4	0.96	±	0.21		86.62	43.31	41.6
2019-02-06	February	HO4_1	HO4	0.16	±	0.00		89.64	44.82	7.0
2019-02-06	February	HO4_2	HO4	0.55	±	0.05		49.72	24.86	13.7
2019-02-13	February	HO4_1	HO4	0.40	±	0.12		27.49	13.75	5.6
2019-02-13	February	HO4_2	HO4	0.17	±	0.07		21.40	10.70	1.9
2019-02-27	February	HO4_1	HO4	1.95	±	0.36		62.60	31.30	60.9
2019-03-14	March	HO4_1	HO4	3.01	±	0.02		72.83	36.42	109.5
2019-03-14	March	HO4_2	HO4	0.56	±	0.11		47.16	23.58	13.3

Date	Month	Plot		Si ±					
2019-03-25	March	HO4_2	HO4	0.86	±	0.03	43.41	21.71	18.7
2019-03-25	March	HO4_1	HO4	0.63	±	0.14	23.71	11.86	7.4
2019-04-01	April	HO4_1	HO4	0.99	±	0.02	34.91	17.46	17.2
2019-04-01	April	HO4_2	HO4	0.47	±	0.25	31.48	15.74	7.5
2019-04-08	April	HO4_1	HO4	0.81	±	0.29	27.29	13.65	11.1
2019-04-08	April	HO4_2	HO4	0.27	±	0.02	38.32	19.16	5.1
2019-04-20	April	HO4_1	HO4	0.66		***	65.94	32.97	21.7
2019-04-20	April	HO4_2	HO4	6.84	±	0.00	46.69	23.35	159.6
2019-04-29	April	HO4_1	HO4	0.66	±	0.00	26.37	13.19	8.7
2019-04-29	April	HO4_2	HO4	0.52	±	0.10	22.49	11.25	5.8
2019-05-07	May	HO4_1	HO4	0.48	±	0.18	20.99	10.50	5.1
2019-05-07	May	HO4_2	HO4	0.51	±	0.04	16.60	8.30	4.3
2019-05-29	May	HO4_1	HO4	0.23	±	0.01	20.55	10.28	2.3
2019-05-29	May	HO4_2	HO4	4.36	±	0.11	28.62	14.31	62.4

410

Table B4 Mean Si concentrations and statistical analyses on log transformed data

Management zone	Water regime		N	Si_M µg g^{-1} soil			Shapiro-Wilk p-value	Levene p-value	Si_{Am} mg g^{-1} soil			Shapiro-Wilk p-value	Levene p-value
Palm circle	Well-drained	HO	4	11.17	±	5.42	0.68		1.71	±	0.35	*0.04ᵃ*	
Oil-palm row	Well-drained	HO	4	6.38	±	2.85	*0.01ᵃ*	0.26	1.87	±	0.51	0.28	0.50
Interrow	Well-drained	HO	3	5.62	±	0.10	0.80		1.88	±	0.39	0.18	
Frond pile	Well-drained	HO	4	13.68	±	6.54	1.00		3.97	±	1.54	0.96	
Palm circle	Riparian	HOr	4	10.55	±	3.06	0.43		1.44	±	0.55	0.87	
Oil-palm row	Riparian	HOr	4	11.94	±	6.09	0.39	0.89	2.08	±	0.17	0.89	0.15
Interrow	Riparian	HOr	4	11.38	±	3.74	0.76		2.71	±	0.29	0.14	
Frond pile	Riparian	HOr	4	19.56	±	6.13	0.65		2.96	±	0.69	0.26	

Mean ± Standard deviation. Statistics was conducted by 1-way ANOVA and Tukey post-hoc test.
Normally distributed data, whereby the homogeneity of variances was asserted.
[a]Italics = homogeneity of variances was not asserted.

7 Data availability

415   Data are provided in the appendix of the manuscript.

8 Supplement

Data are provided in the appendix of the manuscript.

9 Author's contribution

BvL and DS designed the study of the manuscript with input from HH, ST and AT. BG conducted soil sampling

420   with input from BvL, ST, AT, and DS. CS sampled and provided meteorological data. BG conducted laboratory analysis and evaluated the data with input from BvL, HH, CS and DS. BG wrote the first draft. All authors (BG, BvL, HH, CS, ST, AT, and DS) contributed to generating and reviewing the subsequent versions of the paper.

10 Competing interests

The authors declare that they have no conflict of interests.

425   **11 Acknowledgements**

We thank the German Research Foundation DFG for funding this project (DFG project no. 391702217). The project was associated to the Collaborative Research Center 990 "Environmental and Socioeconomic Functions of Tropical Lowland Rainforest Transformation Systems" (CRC 990, DFG project no. 192626868). We also thank the Ministry of Education, Technology and Higher Education (RISTEKDIKTI) for granting a research permission

430   in Indonesia and the CRC 990 oil-palm smallholder partners. Soil sampling was conducted using the research permits 110/SIP/FRP/E5/Dit.KI/IV/2018 and 187/ E5/E5.4/SIP/2019. Special thanks go to our Indonesian counterparts, the CRC-990 office members, and our fieldwork assistants Nando, Daniel, Somad and Firdaus in Jambi. We would also like to thank the laboratory staff from the Institute of Geography, University of Göttingen, Jürgen Grotheer, Anja Södje and Petra Voigt, for their support.

435   **12 Financial support**

This project was funded by the German Research Foundation DFG (DFG project no. 391702217).

13 References

Albert, R. M., Bamford, M. K., and Esteban, I.: Reconstruction of ancient palm vegetation landscapes using a phytolith approach, Quaternary International, 369, 51–66, https://doi.org/10.1016/j.quaint.2014.06.067, 2015.

440   Alexandre, A., Meunier, J.-D., Colin, F., and Koud, J.-M.: Plant impact on the biogeochemical cycle of silicon and related weathering processes, Geochim Cosmochim Acta, 61, 677–682, https://doi.org/10.1016/S0016-7037(97)00001-X, 1997.

Allen, K., Corre, M. D., Kurniawan, S., Utami, S. R., and Veldkamp, E.: Spatial variability surpasses land-use change effects on soil biochemical properties of converted lowland landscapes in Sumatra, Indonesia, Geoderma,

445   284, 42–50, https://doi.org/10.1016/j.geoderma.2016.08.010, 2016.

Arshad, A. M.: Physical land evaluation for oil palm cultivation in district of Temerloh and Kuantan, Pahang, Peninsular Malaysia., Journal of Biology, Agriculture and Healthcare., 5, 104–112, 2015.

Barão, L., Clymans, W., Vandevenne, F., Meire, P., Conley, D. J., and Struyf, E.: Pedogenic and biogenic alkaline-extracted silicon distributions along a temperate land-use gradient, Eur J Soil Sci, 65, 693–705, https://doi.org/10.1111/ejss.12161, 2014.

Barão, L., Teixeira, R., Vandevenne, F., Ronchi, B., Unzué-Belmonte, D., and Struyf, E.: Silicon Mobilization in Soils: the Broader Impact of Land Use, Silicon, 12, 1529–1538, https://doi.org/10.1007/s12633-019-00245-y, 2020.

Blecker, S. W., McCulley, R. L., Chadwick, O. A., and Kelly, E. F.: Biologic cycling of silica across a grassland bioclimosequence, Global Biogeochemical Cycles, 20, https://doi.org/10.1029/2006GB002690, 2006.

Breuning-Madsen, H., Kristensen, J. Å., Awadzi, T. W., and Murray, A. S.: Early cultivation and bioturbation cause high long-term soil erosion rates in tropical forests: OSL based evidence from Ghana, Catena, 151, 130–136, https://doi.org/10.1016/j.catena.2016.12.002, 2017.

Clough, Y., Krishna, V. v., Corre, M. D., Darras, K., Denmead, L. H., Meijide, A., Moser, S., Musshoff, O., Steinebach, S., Veldkamp, E., Allen, K., Barnes, A. D., Breidenbach, N., Brose, U., Buchori, D., Daniel, R., Finkeldey, R., Harahap, I., Hertel, D., Holtkamp, A. M., Hörandl, E., Irawan, B., Jaya, I. N. S., Jochum, M., Klarner, B., Knohl, A., Kotowska, M. M., Krashevska, V., Kreft, H., Kurniawan, S., Leuschner, C., Maraun, M., Melati, D. N., Opfermann, N., Pérez-Cruzado, C., Prabowo, W. E., Rembold, K., Rizali, A., Rubiana, R., Schneider, D., Tjitrosoedirdjo, S. S., Tjoa, A., Tscharntke, T., and Scheu, S.: Land-use choices follow profitability at the expense of ecological functions in Indonesian smallholder landscapes, Nat Commun, 7, 1–12, https://doi.org/10.1038/ncomms13137, 2016.

Clymans, W., Struyf, E., Van den Putte, A., Langhans, C., Wang, Z., and Govers, G.: Amorphous silica mobilization by inter-rill erosion: Insights from rainfall experiments, Earth Surf Process Landf, 40, 1171–1181, https://doi.org/10.1002/esp.3707, 2015.

Comte, I., Colin, F., Whalen, J. K., Grünberger, O., and Caliman, J.-P.: Agricultural practices in oil palm plantations and their impact on hydrological changes, nutrient fluxes and water quality in Indonesia: a review., 71–124 pp., https://doi.org/10.1016/B978-0-12-394277-7.00003-8, 2012.

Conley, D. J., Likens, G. E., Buso, D. C., Saccone, L., Bailey, S. W., and Johnson, C. E.: Deforestation causes increased dissolved silicate losses in the Hubbard Brook Experimental Forest, Glob Chang Biol, 14, 2548–2554, https://doi.org/10.1111/j.1365-2486.2008.01667.x, 2008.

Corley, R. H. v. and Tinker, P. B.: The Oil Palm, Fifth edit., 687 pp., https://doi.org/10.1017/cbo9781316530122.010, 2016.

Cornelis, J., Delvaux, B., Georg, R. B., Lucas, Y., Ranger, J., and Opfergelt, S.: Tracing the origin of dissolved silicon transferred from various soil-plant systems towards rivers: a review, Biogeosciences, 8, 89–112, https://doi.org/10.5194/bg-8-89-2011, 2011.

de Coster, G. L.: The Geology of the central and south sumatra basins, in: IPA, 2006 - 3rd Annual Convention Proceedings, 1974, 77, 2006.

Darras, K. F. A., Corre, M. D., Formaglio, G., Tjoa, A., Potapov, A., Brambach, F., Sibhatu, K. T., Grass, I., Rubiano, A. A., Buchori, D., Drescher, J., Fardiansah, R., Hölscher, D., Irawan, B., Kneib, T., Krashevska, V., Krause, A., Kreft, H., Li, K., Maraun, M., Polle, A., Ryadin, A. R., Rembold, K., Stiegler, C., Scheu, S., Tarigan, S., Valdés-Uribe, A., Yadi, S., Tscharntke, T., and Veldkamp, E.: Reducing Fertilizer and Avoiding Herbicides in Oil Palm Plantations—Ecological and Economic Valuations, Frontiers in Forests and Global Change, 2, 1–15, https://doi.org/10.3389/ffgc.2019.00065, 2019.

Dislich, C., Keyel, A. C., Salecker, J., Kisel, Y., Meyer, K. M., Auliya, M., Barnes, A. D., Corre, M. D., Darras, K., Faust, H., Hess, B., Klasen, S., Knohl, A., Kreft, H., Meijide, A., Nurdiansyah, F., Otten, F., Pe'er, G., Steinebach, S., Tarigan, S., Tölle, M. H., Tscharntke, T., and Wiegand, K.: A review of the ecosystem functions

in oil palm plantations, using forests as a reference system, Biological Reviews, 92, 1539–1569, https://doi.org/10.1111/brv.12295, 2017.

495 Drescher, J., Rembold, K., Allen, K., Beckscha, P., Buchori, D., Clough, Y., Faust, H., Fauzi, A. M., Gunawan, D., Hertel, D., Irawan, B., Jaya, I. N. S., Klarner, B., Kleinn, C., Knohl, A., Kotowska, M. M., Krashevska, V., Krishna, V., Leuschner, C., Lorenz, W., Meijide, A., Melati, D., Steinebach, S., Tjoa, A., Tscharntke, T., Wick, B., Wiegand, K., Kreft, H., and Scheu, S.: Ecological and socio-economic functions across tropical land use systems after rainforest conversion, Philosophical Transactions of the Royal Society B: Biological Sciences, 371, 20150275, https://doi.org/10.1098/rstb.2015.0275, 2016.

500 Dürr, H. H., Meybeck, M., Hartmann, J., Laruelle, G. G., and Roubeix, V.: Global spatial distribution of natural riverine silica inputs to the coastal zone, Biogeosciences, 8, 597–620, https://doi.org/10.5194/bg-8-597-2011, 2011.

Epstein, E.: Silicon: its manifold roles in plants, Annals of Applied Biology, 155, 155–160, https://doi.org/10.1111/j.1744-7348.2009.00343.x, 2009.

505 Euler, M., Schwarze, S., Siregar, H., and Qaim, M.: Oil Palm Expansion among Smallholder Farmers in Sumatra, Indonesia, J Agric Econ, 67, 658–676, https://doi.org/10.1111/1477-9552.12163, 2016.

Formaglio, G., Veldkamp, E., Duan, X., Tjoa, A., and Corre, M. D.: Herbicide weed control increases nutrient leaching as compared to mechanical weeding in a large-scale oil palm plantation, Biogeosciences, 17, 5243–5262, https://doi.org/10.5194/bg-2020-153, 2020.

510 Fox, J. and Weisberg, S.: An {R} Companion to Applied Regression, 2019.

Fraysse, F., Pokrovsky, O. S., Schott, J., and Meunier, J.-D.: Surface chemistry and reactivity of plant phytoliths in aqueous solutions, Chemical Geology, 258, 197–206, https://doi.org/10.1016/j.chemgeo.2008.10.003, 2009.

Georgiadis, A., Sauer, D., Herrmann, L., Breuer, J., Zarei, M., and Stahr, K.: Development of a method for sequential Si extraction from soils, Geoderma, 209, 251–261, https://doi.org/10.1016/j.geoderma.2013.06.023, 515 2013.

Georgiadis, A., Rinklebe, J., Straubinger, M., and Rennert, T.: Silicon fractionation in Mollic Fluvisols along the Central Elbe River, Germany, Catena (Amst), 153, 100–105, https://doi.org/10.1016/j.catena.2017.01.027, 2017.

Grass, I., Kubitza, C., Krishna, V. v., Corre, M. D., Mußhoff, O., Pütz, P., Drescher, J., Rembold, K., Ariyanti, E. S., Barnes, A. D., Brinkmann, N., Brose, U., Brümmer, B., Buchori, D., Daniel, R., Darras, K. F. A., Faust, 520 H., Fehrmann, L., Hein, J., Hennings, N., Hidayat, P., Hölscher, D., Jochum, M., Knohl, A., Kotowska, M. M., Krashevska, V., Kreft, H., Leuschner, C., Lobite, N. J. S., Panjaitan, R., Polle, A., Potapov, A. M., Purnama, E., Qaim, M., Röll, A., Scheu, S., Schneider, D., Tjoa, A., Tscharntke, T., Veldkamp, E., and Wollni, M.: Trade-offs between multifunctionality and profit in tropical smallholder landscapes, Nat Commun, 11, 1–13, https://doi.org/10.1038/s41467-020-15013-5, 2020.

525 Grasshoff, K., Kremling, K., and Ehrhardt, M.: Methods of sea water analysis, third., John Wiley & Sons, 899 pp., https://doi.org/10.1016/0304-4203(78)90045-2, 2009.

Guillaume, T., Damris, M., and Kuzyakov, Y.: Losses of soil carbon by converting tropical forest to plantations: erosion and decomposition estimated by δ13C, Glob Chang Biol, 21, 3548–3560, https://doi.org/10.1111/gcb.12907, 2015.

530 Guillaume, T., Holtkamp, A. M., Damris, M., Brümmer, B., and Kuzyakov, Y.: Soil degradation in oil palm and rubber plantations under land resource scarcity, Agriculture, Ecosystems and Environment, 232, 110–118, https://doi.org/10.1016/j.agee.2016.07.002, 2016.

Guntzer, F., Keller, C., and Meunier, J. D.: Benefits of plant silicon for crops: A review, Agron Sustain Dev, 32, 201–213, https://doi.org/10.1007/s13593-011-0039-8, 2012.

535   Harrison, R. D. and Swinfield, T.: Restoration of logged humid tropical forests: An experimental programme at harapan rainforest, Indonesia, Trop Conserv Sci, 8, 4–16, https://doi.org/10.1177/194008291500800103, 2015.

Haynes, R. J.: A contemporary overview of silicon availability in agricultural soils, Journal of Plant Nutrition and Soil Science, 177, 831–844, https://doi.org/10.1002/jpln.201400202, 2014.

Hennings, N., Becker, J. N., Guillaume, T., Damris, M., Dippold, M. A., and Kuzyakov, Y.: Riparian wetland
540   properties counter the effect of land-use change on soil carbon stocks after rainforest conversion to plantations, Catena (Amst), 196, 104941, https://doi.org/10.1016/j.catena.2020.104941, 2021.

Huisman, S. N., Raczka, M. F., and McMichael, C. N. H.: Palm phytoliths of mid-elevation Andean forests, Frontiers in Ecology and Evolution, 6, 1–8, https://doi.org/10.3389/fevo.2018.00193, 2018.

Iler, R. K.: The chemistry of silica: solubility, polymerization, colloid and surface properties, and biochemistry,
545   Wiley & Sons, 896 pp., https://doi.org/10.1002/ange.19800920433, 1979.

Kassambara, A.: ggpubr: "ggplot2" Based Publication Ready Plots R package version 0.5.0, https://CRAN.R-project.org/package=ggpubr, 2022.

Keller, C., Guntzer, F., Barboni, D., Labreuche, J., and Meunier, J.-D.: Impact of agriculture on the Si biogeochemical cycle: Input from phytolith studies, Comptes Rendus Geoscience, 344, 739–746,
550   https://doi.org/10.1016/j.crte.2012.10.004, 2012.

Klotzbücher, T., Klotzbücher, A., Kaiser, K., Merbach, I., and Mikutta, R.: Impact of agricultural practices on plant-available silicon, Geoderma, 331, 15–17, https://doi.org/10.1016/j.geoderma.2018.06.011, 2018.

Kotowska, M. M., Leuschner, C., Triadiati, T., Meriem, S., and Hertel, D.: Quantifying above- and belowground biomass carbon loss with forest conversion in tropical lowlands of Sumatra (Indonesia), Glob Chang Biol, 21,
555   3620–3634, https://doi.org/10.1111/gcb.12979, 2015.

Kraushaar, S., Konzett, M., and Meister, J.: Suitability of phytoliths as a quantitative process tracer for soil erosion studies, https://doi.org/10.1002/esp.5121, 2021.

Laumonier, Y.: The Vegetation and Physiography of Sumatra, in: Geobotany, vol. 22, Kluwer Academic Publishers, 223, https://doi.org/10.1007/978-94-009-0031-8, 1997.

560   Li, Z., de Tombeur, F., vander Linden, C., Cornelis, J. T., and Delvaux, B.: Soil microaggregates store phytoliths in a sandy loam, Geoderma, 360, 114037, https://doi.org/10.1016/j.geoderma.2019.114037, 2020.

vander Linden, C. and Delvaux, B.: The weathering stage of tropical soils affects the soil-plant cycle of silicon, but depending on land use, Geoderma, 351, 209–220, https://doi.org/10.1016/j.geoderma.2019.05.033, 2019.

von der Lühe, B., Pauli, L., Greenshields, B., Hughes, H. J., Tjoa, A., and Sauer, D.: Transformation of Lowland
565   Rainforest into Oil-palm Plantations and use of Fire alter Topsoil and Litter Silicon Pools and Fluxes, Silicon, 13, 4345–4353, https://doi.org/10.1007/s12633-020-00680-2, 2020.

Luke, S. H., Purnomo, D., Advento, A. D., Aryawan, A. A. K., Naim, M., Pikstein, R. N., Ps, S., Rambe, T. D. S., Soeprapto, Caliman, J.-P., Snaddon, J. L., Foster, W. A., and Turner, E. C.: Effects of understory vegetation management on plant communities in oil palm plantations in Sumatra, Indonesia, Frontiers in Forests and Global
570   Change, 2, 1–13, https://doi.org/10.3389/ffgc.2019.00033, 2019.

Ma, J. F. and Takahashi, E.: Silicon-accumulating plants in the plant kingdom, in: Soil, fertilizer, and plant silicon research in Japan, Elsevier Science, Amsterdam, 63–71, https://doi.org/10.1016/b978-044451166-9/50005-1, 2002.

Meijaard, E., Brooks, T., Carlson, K. M., Slade, E. M., and Ulloa, J. G.: The environmental impacts of palm oil
575   in context, Nat Plants, 6, 1418–1426, https://doi.org/10.1038/s41477-020-00813-w, 2020.

Meunier, J. D., Keller, C., Guntzer, F., Riotte, J., Braun, J. J., and Anupama, K.: Assessment of the 1% Na2CO3 technique to quantify the phytolith pool, Geoderma, 216, 30–35, https://doi.org/10.1016/j.geoderma.2013.10.014, 2014.

580 Munevar, F. and Romero, A.: Soil and plant silicon status in oil palm crops in Colombia, Exp Agric, 51, 382, https://doi.org/10.1017/S0014479714000374, 2015.

Oliveira, P. T. S., Wendland, E., and Nearing, M. A.: Rainfall erosivity in Brazil: a review, Catena (Amst), 100, 139–147, https://doi.org/10.1016/j.catena.2012.08.006, 2013.

Qaim, M., Sibhatu, K. T., Siregar, H., and Grass, I.: Environmental, Economic, and Social Consequences of the Oil Palm Boom, Annu Rev Resour Economics, 12, 1–24, https://doi.org/10.1146/annurev-resource-110119-
585 024922, 2020.

Quigley, K. M., Donati, G. L., and Anderson, T. M.: Variation in the soil 'silicon landscape' explains plant silica accumulation across environmental gradients in Serengeti, Plant and Soil, 410, 217–229, https://doi.org/10.1007/s11104-016-3000-4, 2017.

Revelle, W.: psych: Procedures for Personality and Psychological Research, 2022.

590 Sauer, D., Saccone, L., Conley, D. J., Herrmann, L., and Sommer, M.: Review of methodologies for extracting plant-available and amorphous Si from soils and aquatic sediments, Biogeochemistry, 80, 89–108, https://doi.org/10.1007/s10533-005-5879-3, 2006.

Schaller, J. and Puppe, D.: Heat improves silicon availability in mineral soils, Geoderma, 386, 114909, https://doi.org/10.1016/j.geoderma.2020.114909, 2021.

595 Schaller, J., Frei, S., Rohn, L., and Gilfedder, B. S.: Amorphous silica controls water storage capacity and phosphorus mobility in soils, Front Environ Sci, 8, 94, https://doi.org/10.3389/fenvs.2020.00094, 2020.

Schaller, J., Puppe, D., Kaczorek, D., Ellerbrock, R., and Sommer, M.: Silicon cycling in soils revisited, Plants, 10, 1–36, https://doi.org/10.3390/plants10020295, 2021.

Sinukaban, N., Tarigan, S. D., Purwakusuma, W., Baskoro, D. P. T., and Wahyuni, E. D.: Analysis of watershed
600 function sediment transfer across various type of filter strips, 72 pp., 2000.

Street-Perrott, F. A. and Barker, P. A.: Biogenic silica: a neglected component of the coupled global continental biogeochemical cycles of carbon and silicon, Earth Surf Process Landf, 33, 1436–1457, https://doi.org/10.1002/esp.1712 F., 2008.

Struyf, E. and Conley, D.: Emerging understanding of the ecosystem silica filter, Biogeochemistry, 107, 9–18,
605 https://doi.org/10.1007/s10533-011-9590-2 SYNTHESIS, 2012.

Struyf, E. and Conley, D. J.: Silica: an essential nutrient in wetland biogeochemistry, Front Ecol Environ, 7, 88–94, https://doi.org/10.1890/070126, 2009.

Struyf, E., Smis, A., Van Damme, S., Garnier, J., Govers, G., Van Wesemael, B., Conley, D. J., Batelaan, O., Frot, E., Clymans, W., Vandevenne, F., Lancelot, C., Goos, P., and Meire, P.: Historical land use change has
610 lowered terrestrial silica mobilization, Nat Commun, 1, 1–7, https://doi.org/10.1038/ncomms1128, 2010.

Tarigan, S., Stiegler, C., Wiegand, K., Knohl, A., and Murtilaksono, K.: Relative contribution of evapotranspiration and soil compaction to the fluctuation of catchment discharge: case study from a plantation landscape, Hydrological Sciences Journal, 65, 1239–1248, https://doi.org/10.1080/02626667.2020.1739287, 2020.

615 de Tombeur, F., Turner, B. L., Laliberté, E., Lambers, H., Mahy, G., Faucon, M. P., Zemunik, G., and Cornelis, J. T.: Plants sustain the terrestrial silicon cycle during ecosystem retrogression, Science (1979), 369, 1245–1248, https://doi.org/10.1126/science.abc0393, 2020.

Tsujino, R., Yumoto, T., Kitamura, S., Djamaluddin, I., and Darnaedi, D.: History of forest loss and degradation in Indonesia, Land use policy, 57, 335–347, https://doi.org/10.1016/j.landusepol.2016.05.034, 2016.

620 Unzué-Belmonte, D., Ameijeiras-Mariño, Y., Opfergelt, S., Cornelis, J. T., Barão, L., Minella, J., Meire, P., and Struyf, E.: Land use change affects biogenic silica pool distribution in a subtropical soil toposequence, Solid Earth, 8, 737–750, https://doi.org/10.5194/se-8-737-2017, 2017.

Vandevenne, F., Struyf, E., Clymans, W., and Meire, P.: Agricultural silica harvest: have humans created a new loop in the global silica cycle?, Front Ecol Environ, 10, 243–248, https://doi.org/10.1890/110046, 2012.

625 Wickham, H.: ggplot2: Elegant Graphics for Data Analysis, 2016.